Gene Copy-Number Variation in Haploid and Diploid Strains of the Yeast *Saccharomyces cerevisiae*

Hengshan Zhang,*[,1] Ane F. B. Zeidler,[†] Wei Song,* Christopher M. Puccia,[†] Ewa Malc,[‡] Patricia W. Greenwell,* Piotr A. Mieczkowski,[‡] Thomas D. Petes,* and Juan Lucas Argueso[†,2]

*Department of Molecular Genetics and Microbiology, Duke University Medical Center, Durham, North Carolina 27710, [†]Department of Environmental and Radiological Health Sciences, Colorado State University, Fort Collins, Colorado 80523, and [‡]Lineberger Comprehensive Cancer Center, Carolina Center for Genome Science, Department of Genetics, University of North Carolina, Chapel Hill, North Carolina 27599

ABSTRACT The increasing ability to sequence and compare multiple individual genomes within a species has highlighted the fact that copy-number variation (CNV) is a substantial and underappreciated source of genetic diversity. Chromosome-scale mutations occur at rates orders of magnitude higher than base substitutions, yet our understanding of the mechanisms leading to CNVs has been lagging. We examined CNV in a region of chromosome 5 (chr5) in haploid and diploid strains of *Saccharomyces cerevisiae*. We optimized a CNV detection assay based on a reporter cassette containing the *SFA1* and *CUP1* genes that confer gene dosage-dependent tolerance to formaldehyde and copper, respectively. This optimized reporter allowed the selection of low-order gene amplification events, going from one copy to two copies in haploids and from two to three copies in diploids. In haploid strains, most events involved tandem segmental duplications mediated by nonallelic homologous recombination between flanking direct repeats, primarily Ty1 elements. In diploids, most events involved the formation of a recurrent nonreciprocal translocation between a chr5 Ty1 element and another Ty1 repeat on chr13. In addition to amplification events, a subset of clones displaying elevated resistance to formaldehyde had point mutations within the *SFA1* coding sequence. These mutations were all dominant and are proposed to result in hyperactive forms of the formaldehyde dehydrogenase enzyme.

As a consequence of studies that utilize genomic microarrays and next-generation DNA sequencing, it has become clear that much of the natural genetic variation that exists between individuals is due to alterations in the number of copies of genes rather than differences in the nucleotide sequence (Girirajan *et al.* 2011; Veltman and Brunner 2012). It has been calculated that 8–25 kb of DNA are deleted or duplicated per generation in humans compared to about 100 bp of point mutations (Itsara *et al.* 2010). Although deletions and duplications vary in size from a few base pairs (for example, changes in the lengths of microsatellites) to many megabases (for example, changes in ploidy), Girirajan *et al.* (2011) define copy-number variants (CNVs) in humans as changes that vary in size between 50 bp and 1 Mb. While most CNV events have no obvious effect, a significant number are associated with human diseases including Charcot–Marie–Tooth syndrome, autosomal dominant leukodystrophy, Williams syndrome, several cancer predispositions, and autism-related and other neurodevelopmental disorders (Abrahams and Geschwind 2008; Girirajan *et al.* 2011; Krepischi *et al.* 2012; Malhotra and Sebat 2012; Sullivan *et al.* 2012). There is also strong evidence suggesting that CNVs played a significant role in human evolution (Iskow *et al.* 2012). Finally, multiple somatic CNV events are frequently observed in the altered karyotypes of cancer cells (Stratton *et al.* 2009).

CNVs have also been widely observed in natural populations and have been studied in detail in model organisms. In the discussion below, we analyze genomic deletions and duplications in the yeast *Saccharomyces cerevisiae*. We define a CNV as a deletion or duplication that includes at least one gene (average of about 2 kb) and no more than one chromosome arm

doi: 10.1534/genetics.112.146522
Manuscript received October 12, 2012; accepted for publication December 17, 2012
Supporting information is available online at http://www.genetics.org/lookup/suppl/doi:10.1534/genetics.112.146522/-/DC1.
[1]Present address: The First Affiliated Hospital of Fujian Medical University, Fuzhou, People's Republic of China.
[2]Corresponding author: 493 MRB Building, 1618 Campus Delivery, Colorado State University, Fort Collins, CO 80523. E-mail: lucas.argueso@colostate.edu

(average of about 400 kb). The most frequently observed mechanisms for the generation of deletions and duplications are illustrated in Figure 1.

Perhaps the most notable early example of CNV in yeast was the discovery of a large deletion on the right arm of chromosome 3 (chr3) that spanned the mating-type locus and distal genes linked to it (Hawthorne 1963). Later studies demonstrated that this ~100-kb deletion was mediated by homologous recombination between two directly oriented nontandem repeats at the *MAT* and *HMR* loci (Herskowitz 1988). The Hawthorne deletion was unusual in that it was originally isolated in a diploid strain. In contrast, most early deletion studies were performed in haploids. As a result, the identified deletions typically involved small segments spanning only a few loci, since larger deletions often include essential genes. For the well-characterized *HIS4* and *CYC1* genes, only a small fraction (<1%) of the mutations were deletions (Fink and Styles 1974; Sherman *et al.* 1974), which occurred at these loci at a frequency $<10^{-8}$/cell division.

Strain-specific hotspots for deletions were identified at two genetic locations. Although deletions of *CYC1* are observed at very low frequency in most wild-type strains, Liebman and colleagues (Liebman *et al.* 1979) found a strain in which deletions of three linked genes (one of which was *CYC1*) occurred at a relatively high rate (10^{-5}–10^{-6} events/division). Subsequently, it was shown that in strains that had a high deletion rate, the *CYC1* gene was flanked by two 6-kb Ty retrotransposons in direct orientation and that the deletion events were a consequence of homologous recombination between the Ty elements (Liebman *et al.* 1981). Similarly, recombination between flanking delta LTR elements (the long-terminal-repeat sequences associated with Ty1 and Ty2 elements) was implicated in the high frequency of deletions at the *SUP4* locus (Rothstein *et al.* 1987). These deletions could reflect single-strand annealing between the direct-flanking repeats (Figure 1A) or represent one of the products of unequal crossing over (Figure 1B).

Assay systems have been developed to study the environmental and genetic control of deletions in yeast. One such assay was developed to study deletions mediated by homologous recombination between direct flanking repeats (DEL assay) (Schiestl 1989). In this system, recombination between two directly repeated mutant *his3* genes, one with a deletion at the 5′ end and one with a deletion at the 3′ end, produced a functional copy of *HIS3* at a very high frequency (10^{-4}/division). In contrast, a different deletion selection system that relied on recombination between micro- or nonhomologous sequences to reactivate a mutant *ura2* gene yielded recombinants at a much lower frequency (10^{-10}/division) (Tourrette *et al.* 2007).

Chen and Kolodner (1999) developed an assay for detecting large deletions involving simultaneous loss of two counterselectable markers (*URA3* and *CAN1*) located ~10 kb apart (gross chromosomal rearrangements, GCR, assay). These markers were located near the left end of chr5, about 10 kb distal to *PCM1*, the first essential gene on the chromosome. The types of genetic events detected by this assay include interstitial deletions, terminal deletions followed by telomere addition, and translocations between chr5 and other chromosomes (Chen and Kolodner 1999). For both the translocations and interstitial deletions, the rate of events in a wild-type strain is very low ($<10^{-9}$/division); the breakpoints of the events occur between *CAN1* and *PCM1* and typically involved micro- or no sequence homology. Most of these rearrangements reflect nonhomologous end-joining (NHEJ) events, although homologous-recombination (HR) events involving very small homologies are also observed (Putnam *et al.* 2005). More recent versions of the GCR assay showed that the introduction of homology either from a dispersed repeated gene family member (*HXT13*) or from a Ty element inserted between *CAN1* and *PCM1* elevated the rate of *URA3*–*CAN1* codeletions by two to three orders of magnitude. Most of these deletions were a consequence of nonreciprocal translocations between the repeat on chr5 and a homologous sequence elsewhere in the genome and were associated with amplification of the terminal segment of the donor chromosome (Figure 1D) (Putnam *et al.* 2009; Chan and Kolodner 2011, 2012). In summary, the frequency of deletions in yeast is highly dependent on the context of the reporter gene. In regions in which the reporter is flanked by directly repeated sequences, deletions are frequent and occur through homologous recombination; in regions without repeats, deletions are rare and often involve NHEJ or other microhomology pathways.

Although duplication events in yeast have been less investigated than deletions, there appear to be more diverse types of mechanisms involved. One distinction between duplication events is whether they involve an increase in copy number of a preexisting duplication or duplication of a sequence that is initially present in single copy. Alterations in copy number of the tandemly repeated ribosomal RNA (rRNA) genes or *CUP1* genes represent the first class of events. For these types of genes, alterations in copy number occur as a consequence of HR of a variety of types including unequal crossovers (Petes 1980; Szostak and Wu 1980; Welch *et al.* 1990), gene conversion (Welch *et al.* 1990; Gangloff *et al.* 1996), and single-strand annealing (SSA) (Ozenberger and Roeder 1991). Some of these events are remarkably frequent. For example, unequal crossovers within the rRNA gene array occur at a frequency of at least 10^{-2}/mitotic division (Szostak and Wu 1980) and a frequency of $\sim10^{-1}$/meiotic division (Petes 1980).

In contrast, the frequency of duplicating sequences that are initially present in single copy is much lower, although very dependent on chromosome context and ploidy. A number of reporter systems have been used to detect duplications; differences in the types of events recovered are likely to reflect the chromosome context of the reporter gene rather than the reporter gene *per se*. Duplications of the *ADH2* or *ADH4* genes can be selected on medium containing antimycin A (Dorsey *et al.* 1992). Duplications of *RPL20B* can be selected as

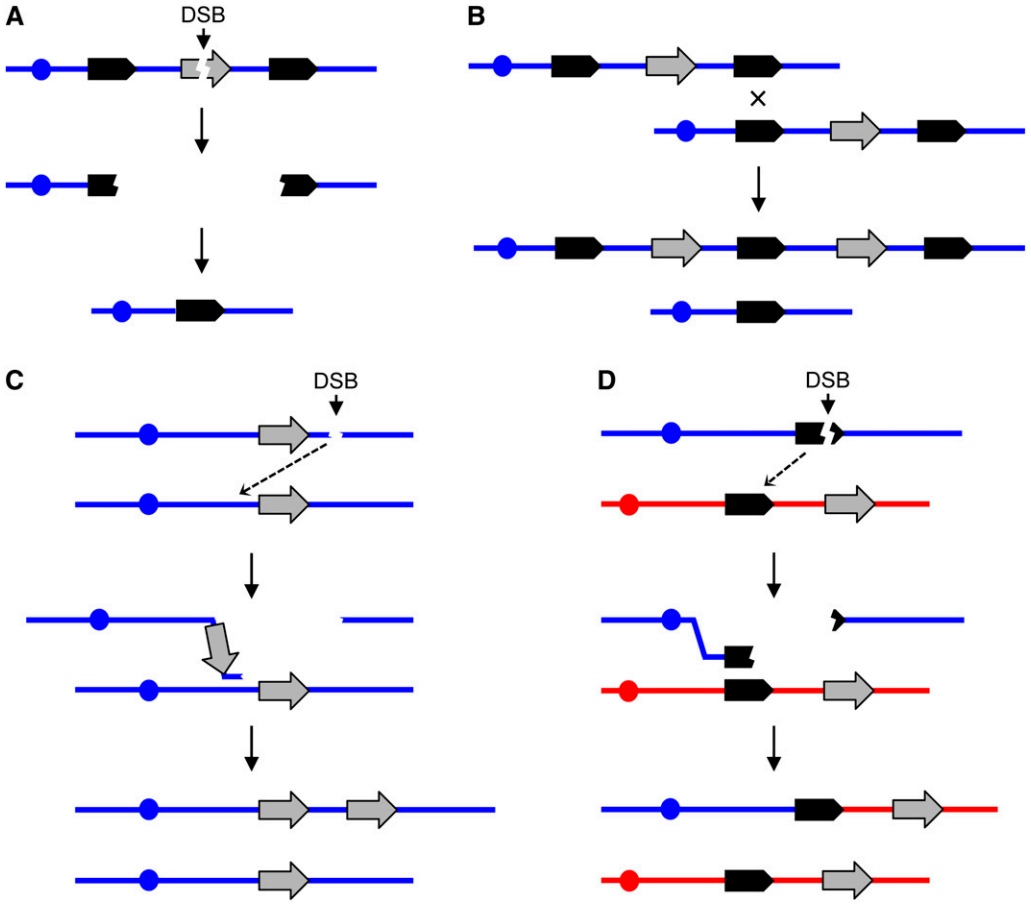

Figure 1 General mechanisms for the generation of deletions and duplications. In this figure, chromosomes are shown as horizontal blue or red lines, DNA repeats as solid arrows, reporter genes as shaded arrows, and centromeres as circles. Single DNA strands are not represented. Variations of these models are also possible. (A) Deletion formation by the single-strand annealing (SSA) pathway. A double-strand DNA break (DSB) between the flanking repeats results in two broken ends that are resected 5′ to 3′. When complementary single-strand regions of the flanking repeats are exposed, reannealing occurs, resulting in loss of the sequences between the repeats (Paques and Haber 1999). (B) Unequal crossovers resulting in deletions and duplications. This homologous recombination event could involve either sister chromatids in haploids or diploids or homologous chromosomes in diploids. (C) Microhomology-mediated replication. A free 3′ end associated with centromere-containing DNA fragment invades a sister chromatid or a homologous chromosome using a nonallelic microhomology sequence. The subsequent break-induced replication (BIR) event generates a duplication in which the breakpoints share little sequence homology. It is assumed that the DNA fragment without a centromere is lost. (D) Coupled terminal duplication and deletion resulting in a nonreciprocal translocation. The different homologs are shown in blue and red. A DSB in or distal to a repeat in the blue chromosome is repaired by a BIR event using a repeat on a nonhomologous chromosome (red). This event results in a duplication of sequences from the red chromosome and a deletion of sequences from the blue chromosome.

normal-growing derivatives that display a rescue of the slow-growth phenotype of their *rpl20AΔ* progenitor strain (Koszul *et al.* 2004; Payen *et al.* 2008), and duplications of a segment of the *ura2-15-30-72* allele can be recovered as Ura$^+$ revertants (Schacherer *et al.* 2005, 2007). Narayanan *et al.* (2006), through an approach similar to the one used in the present study, identified cells with amplification of a cassette containing *CUP1* and *SFA1*, using sequential selection on medium that contained high levels of copper and formaldehyde. Finally, high-order amplification (>10 extra copies) of the partly defective *leu2-d* allele can be selected as Leu$^+$ prototrophs (Erhart and Hollenberg 1983; Watanabe and Horiuchi 2005). A duplication screening system has also been developed based on the color displayed by cells carrying one (pink) or two or more copies (red) of the *ade3-2p* reporter gene (Koshland *et al.* 1985; Green *et al.* 2010).

Less specific selection regimens also have been used to obtain duplications. For example, growth of yeast cells in medium with low levels of phosphate result in duplication of the linked *PHO3* and *PHO5* genes (Hansche *et al.* 1978), cells grown in limited glucose have duplications of the hexose transporter encoded by *HXT6* (Brown *et al.* 1998; Dunham *et al.* 2002), and cells selected in medium with low sulfur concentrations amplified the *SUL1* gene (Gresham *et al.* 2008). Amplification of the *HTA2–HTB2* histone genes has also been identified as a dosage compensation mechanism for the deletion of *HTA1–HTB1* (Libuda and Winston 2006). Finally, duplications (and deletions) in yeast have been detected without any selection in irradiated diploids (Argueso *et al.* 2008), in strains with an HO-induced DNA break (Hoang *et al.* 2010), and in genetically unstable *tel1 mec1* strains (Vernon *et al.* 2008; McCulley and Petes 2010).

The types of duplications commonly observed can be classified into six groups: (1) interstitial segmental duplications in which the breakpoints are in repeated sequences in direct orientation (Koszul *et al.* 2004; Libuda and Winston 2006; Argueso *et al.* 2008; Payen *et al.* 2008; McCulley and Petes 2010); (2) segmental duplications unassociated with repeats at the duplication breakpoints (Koszul *et al.* 2004; Schacherer *et al.* 2005, 2007; Payen *et al.* 2008); (3) interstitial duplications in which the duplicated segments are in an inverted orientation (Moore *et al.* 2000; Rattray *et al.* 2005; Watanabe and Horiuchi 2005; Narayanan *et al.* 2006); (4) terminal duplications of part of one chromosome

arm associated with a terminal deletion of another chromosome (Dunham *et al.* 2002; Umezu *et al.* 2002; Argueso *et al.* 2008; Kim *et al.* 2008; Vernon *et al.* 2008; Hoang *et al.* 2010; McCulley and Petes 2010; Chan and Kolodner 2011, 2012); (5) linear extrachromosomal plasmids with the amplified copies in inverted orientation (Dorsey *et al.* 1992; Narayanan *et al.* 2006); and, (6) interstitial triplications of a genomic segment containing an origin of replication flanked by short inverted repeats (Brewer *et al.* 2011).

Class 1 duplications can be generated by unequal crossovers (Figure 1B) or by break-induced replication (BIR) in which a double-strand break (DSB) in one repeat is repaired using a nonallelic repeat on a sister chromatid or a homolog. In one system (Payen *et al.* 2008), duplications of this type were dependent on Pol32p, arguing that these events occurred by BIR. Class 2 duplications are likely to reflect BIR events in which the invading end utilizes very small (<10 bp) regions of homology (Figure 1C) (Schacherer *et al.* 2005, 2007; Payen *et al.* 2008); such events have been termed "microhomology-induced replication" (Hastings *et al.* 2009). Class 3 duplications are associated with the processing or replication of inverted repeats located near the reporter gene. In one study, the initiating event is likely to be processing of a cruciform (Narayanan *et al.* 2006). Most class 4 events are a consequence of a DSB within or near a repeat that is repaired by a BIR event involving a repeat located elsewhere in the genome (resulting in a translocation as in Figure 1D). Since the net result of the translocation event is a large terminal deletion of one chromosome arm and a large duplication of another chromosome arm, class 4 events are more often observed in diploid strains (Dunham *et al.* 2002; Umezu *et al.* 2002; Argueso *et al.* 2008; Kim *et al.* 2008; Vernon *et al.* 2008; Hoang *et al.* 2010; McCulley and Petes 2010). In haploids, only repeats very close to the end of chromosomes can support this type of event (Putnam *et al.* 2009; Chan and Kolodner 2011, 2012). In the two class 5 events analyzed, the reporter genes were located near the telomeres (Dorsey *et al.* 1992; Narayanan *et al.* 2006). The formation of the palindromic plasmid in one system reflected the processing of a small palindromic repeat located centromere proximal to the reporter gene (Narayanan *et al.* 2006). Finally, class 6 inverted triplication events observed at the *SUL1* locus have been proposed to occur through the extrusion of a circular DNA intermediate formed during replication, followed by reintegration into the genome via homologous recombination (Brewer *et al.* 2011).

In summary, there are a variety of mechanisms that produce and select for CNVs in *S. cerevisiae*. The relative importance of these mechanisms is dependent on the chromosome context (in particular, whether the reporter gene is flanked by repeats) and ploidy. In our study, we optimized a system to select for low-order amplification events (one extra copy) that more closely resemble the duplications associated with human disease. We used this system to examine gene duplications in both haploids and diploids and in wild-type and mismatch-repair defective strains. In the chromosome context that we examined (reporter gene in the middle of the right arm of chr5), most duplications reflected homologous recombination between flanking Ty repeats in haploids, whereas diploids displayed mostly nonreciprocal translocations between Ty elements on chr5 and Ty elements on other chromosomes, particularly chr13.

Materials and Methods

Yeast strains and plasmids

All strains used in the CNV assay were isogenic with strain MS71, except for noted locus-specific changes introduced by transformation (Lemoine *et al.* 2005). Allele combinations were obtained by mating isogenic haploid strains of opposite mating types and selecting segregant spores with the desired genotypes. MS71 is essentially isogenic to the CG379 strain background (Morrison *et al.* 1991; Argueso *et al.* 2008). The specific strains and oligonucleotides used in this study are listed in supporting information, Table S1 and Table S2, respectively. A detailed description of the constructions of specific strains and plasmids is presented in File S1.

Culture media and CNV selection conditions

Unless otherwise noted, yeast cells were grown in YPD-rich media or in SC drop-out media (Rose *et al.* 1990). The selection of clones carrying amplification events was performed by first streaking cells to single colonies in YPD plates (2 days, 30°), and then inoculating these colonies in 5 ml liquid YPD (18 hr, 30°). Dilutions containing $\sim 2 \times 10^6$ cells from these cultures were plated on SC supplemented with a complete drop-out mix, 150 μM $CuSO_4$, and 1 mM formadehyde. Formadehyde is not stable in aqueous solution; therefore, 1 M dilutions [813 μl of 37% methanol stabilized stock (Fischer Scientific BP-531) in 9.187 ml of sterile water] were prepared fresh for each batch of media and mixed in immediately before pouring the plates. Plates were always used within 24 hr of pouring. Cells were incubated in this media at 30° and FA/Cu-resistant colonies were observed after 3–5 days. Only one colony per culture was examined in downstream experiments to ensure independence. Candidate CNV clones (CFRs) were streaked to single colonies nonselectively in YPD without FA or Cu for 2 days, and then the purified clones were patched in YPD, grown overnight, and then frozen. The FA/Cu-resistance phenotype of each clone was retested by growing overnight cultures in 5 ml liquid YPD, and then serial dilutions from the cultures were spotted on to SC-complete Cu 150 μM/FA 1 mM alongside their corresponding parental strain. Plates were incubated at 30° for 4 days before the differential growth phenotype was assessed.

The nature of the chromosomal rearrangements present in the selected CFR clones was determined using a molecular karyotype analysis, including PFGE and array CGH, as described previously (Argueso *et al.* 2008). The detailed procedures are presented in File S1. The full set of copy-number

variation events detected by array CGH in all clones examined is shown in Figure S1.

Analysis of loss-of-heterozygosity

Independent clones derived from MS71xYJM789 hybrid background diploids carrying allelic mitotic recombination products resulting in loss-of-heterozygosity (LOH) on the right arm of chr13 were selected in SC-complete plates with 5-FOA. The LOH breakpoints were analyzed from two sets of clones. The first set of 5-FOA-resistant clones was derived from strain JAY408 and was analyzed with custom SNP genotyping microarrays and data analysis methods described previously (St Charles *et al.* 2012). We also isolated a second set of LOH clones derived from strain JAY800. This strain was the one used to measure the rate of LOH on the right arm of chr13, by counting colonies growing in 5-FOA (nonpermissive) and in SC complete (permissive) and by using the values in calculations through the method of the median (Lea and Coulson 1949). LOH breakpoints from this set were analyzed by PCR and restriction fragment length polymorphisms at *Eco*RI (primers JAO1031/JAO1032) and *Bgl*II (primers JAO1029/JAO1030) as described in *Results*.

Results

A new selection system for CNV

De novo CNV is a pervasive source of genetic diversity that has been increasingly associated with phenotypic consequences in humans, including disease. We set out to develop a new assay system to detect chromosomal rearrangements involving *de novo* gene amplification in yeast, especially those events resulting in only one additional copy of the affected genomic segments. To do this, we took advantage of a previous system that used the *SFA1* and *CUP1* genes to detect amplification through their gene dosage-dependent phenotypes. *SFA1* encodes formaldehyde dehydrogenase, which detoxifies formaldehyde (FA), and *CUP1* encodes methallothionein, which sequesters copper ions (Cu) from solution. Cells harboring amplification of these genes display increased tolerance to formaldehyde and copper, respectively, and these phenotypes have been used to select for gene amplification (Narayanan *et al.* 2006). A limitation of this earlier system, however, was that it primarily identified clones carrying multiple copies of the reporter genes (>10-fold increase in some cases) because the difference in phenotype between amplification levels was subtle. We therefore decided to optimize the selection conditions with the goal of identifying clones with genome rearrangements that more closely resembled those seen in human *de novo* CNV (*i.e.*, only one extra copy of the amplified genes).

We first deleted the endogenous copy of *SFA1* and its regulatory regions, and we also removed the entire cluster of tandem *CUP1* repeats. Next, we constructed a CNV reporter cassette containing one copy of the *SFA1* and *CUP1* genes, as well as a selective marker for integration (*Hph*, resulting in hygromycin B resistance). This cassette was integrated on chr5 (Figure 2A) between the *DDI1* and *UBP5* genes. This region is also flanked by the *YERCTy1-1* and *YERCTy1-2* repetitive elements that we had previously shown to be the most active for the formation of CNV-associated nonallelic homologous recombination (NAHR) chromosomal rearrangements following induction of DNA DSBs by ionizing radiation (Argueso *et al.* 2008). This region, and the *YERCTy1-1* element in particular, had also been shown by other studies to frequently participate in NAHR under various conditions, including spontaneous rearrangements (Narayanan *et al.* 2006; McCulley and Petes 2010; Chan and Kolodner 2011, 2012; Cheng *et al.* 2012).

Previous studies that used *SFA1* and/or *CUP1* as amplification reporters used either single or sequential selection for resistance to FA or Cu. Given that these genetic resistance mechanisms are completely independent of each other, we reasoned that simultaneous selection for FA and Cu might create a synergistic effect that would provide a more discrete phenotypic differential between strains carrying one, two, or three copies of the reporter. To test this hypothesis, we built both haploid and diploid strains carrying known numbers of reporter insertions either at the chr5 site described above or on chr4, at the native *SFA1* locus. These strains were then tested in media containing incremental concentrations of FA and Cu at various combinations to identify optimal conditions that would inhibit the growth of haploid cells carrying one copy of the reporter, but allow normal growth of cells carrying two or more copies. Likewise, we looked for a combination of FA and Cu that inhibited the growth of diploid cells carrying two homozygous copies of the reporter, but supported growth of cells carrying three or more copies. Representative FA/Cu concentration optimization assays showing the gene dosage-dependent resistance phenotype are presented in Figure S2 and Figure S3. We found that haploid cells with one copy of the reporter had a similar level of FA/Cu resistance as diploids carrying two homozygous copies and that minimal media containing 1.0 mM FA and 150 μM $CuSO_4$ prevented colony formation by these strains. However, this inhibition could be reliably maintained only below a critical plating density of ~200 cells/mm^2, or ~10^6 cells per standard Petri dish. Above this cell concentration, we observed sporadic growth of small background colonies, possibly due to a filtering effect by the excess stagnant cells.

Once the optimal conditions for simultaneous FA/Cu selection had been established, we set out to isolate clones carrying spontaneous chr5 amplification events. We grew cultures of the haploid and diploid test strains, plated appropriate dilutions on FA/Cu, and incubated them for 4 days at 30° to select for spontaneous copy-number variants. To ensure independence, we selected only one FA/Cu resistant colony from each culture, and isolated single-colony derivatives of these strains using rich media without FA/Cu. These purified candidate clones were named CFR (for copper formaldehyde resistant) and were retested in media containing FA/Cu comparing their phenotype to that of

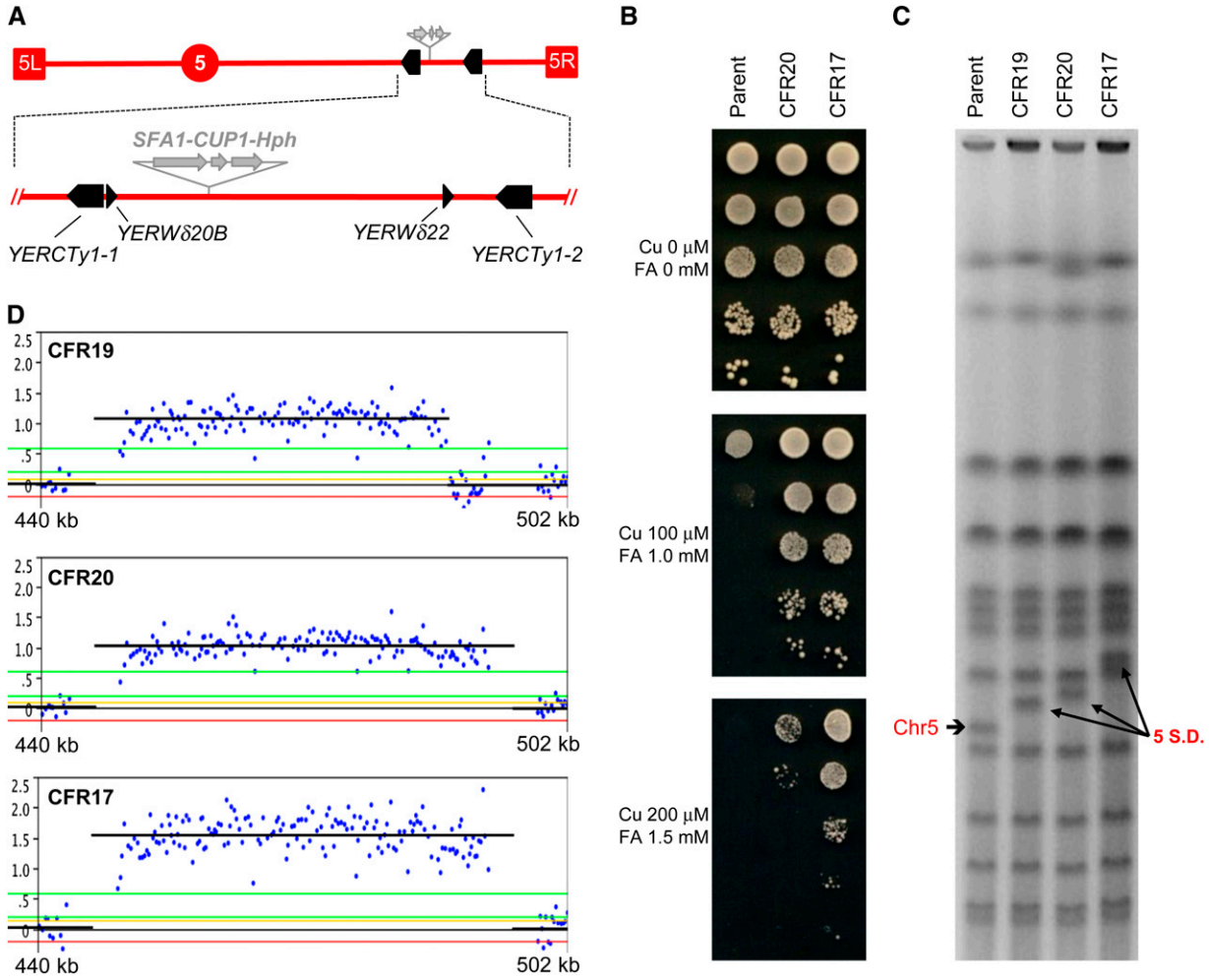

Figure 2 Identification of chr5 amplifications in haploids: Segmental duplications. (A) Schematic representation of the region of chr5 where the *SFA1–CUP1* CNV reporter was inserted (shaded arrows). The reporter also contained a drug-resistance marker, either *Hph* (hygromycin B), as shown, or *Kan* (G418–geneticin). Terminal boxes correspond to the left and right chr5 telomeres (5L and 5R, respectively), and the circle represents *CEN5*. Bottom, expanded view of the region involved in segmental amplifications (440–502 kb), showing full-length Ty1 elements as solid arrows and solo LTRs as arrowheads according to their orientation. (B) FA/Cu-resistance phenotypic differential between the parental haploid strain (JAY372) containing one copy of the reporter and CFR clones carrying two (CFR20) or three (CFR17) copies. Serial dilutions of these strains were spotted on plates containing Cu and FA at the concentrations indicated to the left. (C) PFGE showing the karyotypes of the parental haploid and three CFR clones carrying different segmental amplifications on chr5. The parental size chr5 is indicated to the left and the segmental amplifications are indicated to the right (5 SD). (D) Detailed view of chr5 array-CGH plots showing the Log_2 Cy5/Cy3 signal intensity (copy number) and the rearrangement breakpoints for the three CFRs from C. The plots are aligned directly below to the expanded section of A such that the breakpoints correspond to the repeat sequences. Each blue dot corresponds to the signal of a specific probe in the region. The black horizontal lines correspond to the average signal for probes in a region of amplification. Neutral signal corresponds to no copy-number change (1× in haploids); positive signals corresponding to two copies (~1.0) or three copies (~1.5) are shown.

the respective parent strain (Figure 2B and Figure 3A). The majority of the clones retested positive (102 resistant of 115 CFRs in the full strain set; Table 1), confirming that the selection conditions worked as intended. Even though the sporadic growth of background colonies on densely plated cultures prevented us from calculating high confidence CNV mutation rates, we estimated that gene amplification on chr5 occurred spontaneously at a rate ranging from 10^{-6} to 10^{-7} events/cell division. We focused the remainder of our study on the characterization of the spectra of chromosomal rearrangements associated with the various experimental conditions described below.

Characterization of gene amplification chromosomal rearrangements

After confirming the resistance phenotype, we analyzed all CFR clones for possible chromosome size changes using pulsed-field gel electrophoresis (PFGE). Among the haploid CFRs, we observed loss of the parental-sized chr5 coupled with the appearance of larger new chromosomal bands (Figure 2C). In addition, we also analyzed several CFRs by array CGH to directly test whether the FA/Cu-resistance phenotype was due to CNV (Figure 2D). As expected, most CFRs had additional copies of the chr5 region where the CNV reporter had been inserted. The parallel analysis of

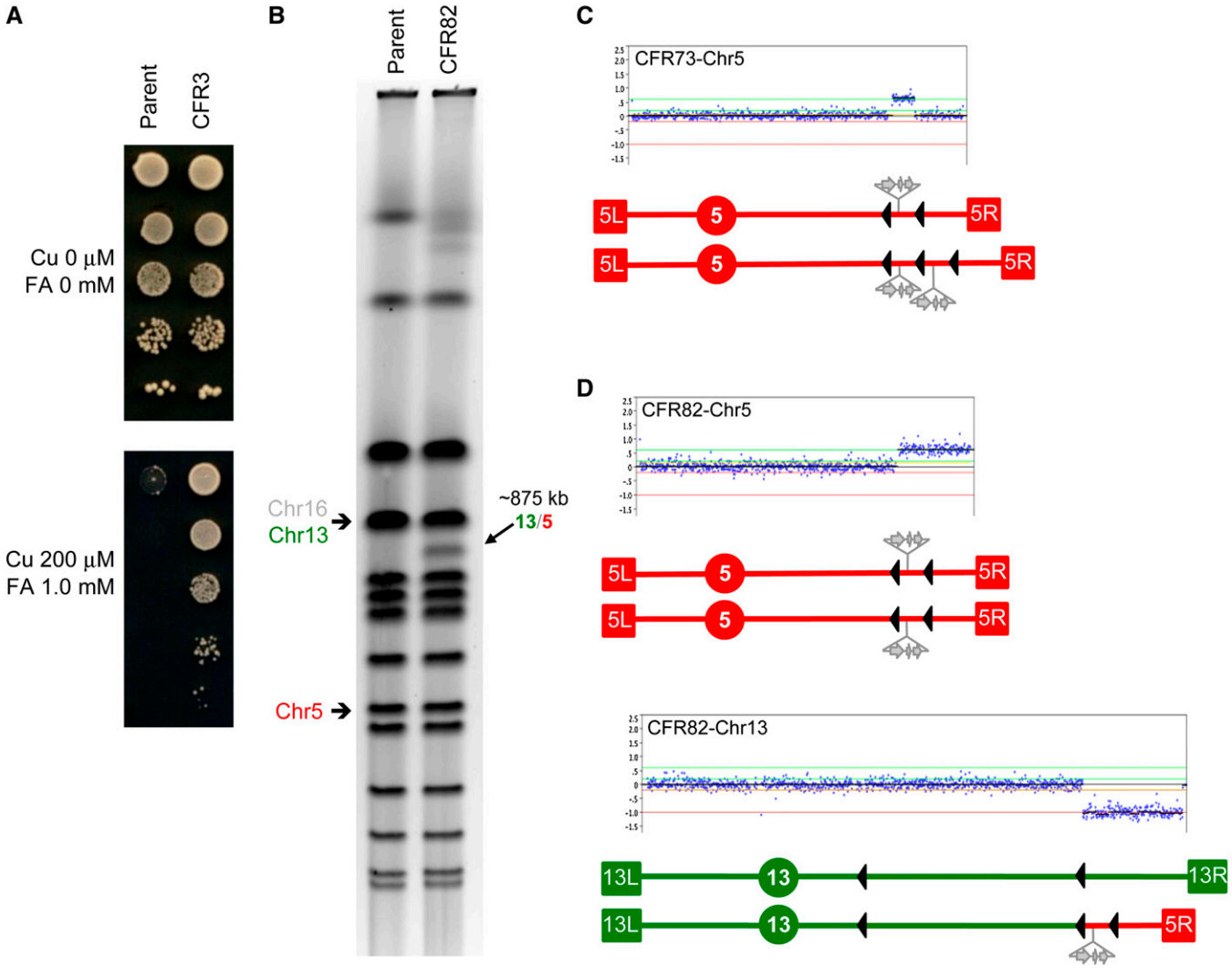

Figure 3 Identification of chr5 amplifications in diploids: chr13/chr5 translocation. Schematic representations are as in Figure 2. Chr5 is shown in red and chr13 is shown in green. (A) FA/Cu-resistance phenotype in the parental diploid strain JAY350 (two reporter copies) compared to a derivative resistant clone CFR3 (three copies). (B) PFGE showing the karyotype of the parental diploid strain JAY350 and of the derivative resistant clone CFR82 carrying the indicated recurrent 875 kb chr13/chr5 translocation. An identical translocation was also present in clone CFR3 shown in A. The parental size chr5 and chr13 are indicated to the left; chr16 comigrates with chr13 and is also indicated. (C) chr5 array-CGH plot (top) and schematic representation (bottom) of the karyotype in the CFR75 clone showing one parental size homolog and one homolog containing a segmental duplication between the *YERCTy1-1* and *YERCTy1-2* elements (solid arrowheads). (D) Array-CGH plots and schematic representation of chr5 and chr13 in the CFR82 clone. The breakpoints correspond to *YERCTy1-1* in chr5 and *YMRCTy1-5* in chr13. For position reference, the chr13 centromere-proximal (left) element *YMRCTy1-4* is also represented (see also Figures 4C and 5B).

the PFGE and array-CGH data showed that in haploids the CNV events were all segmental duplications and that the rearrangement breakpoints were two flanking Ty1 elements or flanking delta elements (the long-terminal repeats associated with Ty1) (Figure 2, A and D and Figure S1). For example, clone CFR19 had breakpoints at the Watson-oriented LTR elements *YERWdelta20B* and *YERWdelta22*, while CFR20 had breakpoints at the Crick-oriented full-length Ty1 elements *YERCTy1-1* and *YERCTy1-2*. The size increases in the chromosomal molecules carrying these two segmental duplications (~40 and ~50 kb, for CFR19 and CFR20, respectively), and the $\log_2$ Cy5/Cy3 amplification signals (+1.07 and +1.09, for CFR19 and CFR20, respectively) were consistent with a doubling of the amplified chr5 region mediated by NAHR between the direct repeats.

Another class of rearrangements observed was exemplified by the pattern seen in CFR17. In this case, the breakpoints were exactly the same as in CFR20, but the rearranged chromosome was ~100 kb longer than the parental chr5, and the array-CGH amplification signal was also higher (Log_2 ratio of +1.57). This result confirmed that CFR17 contained a segmental triplication, mediated by the two Ty1 elements in the region. Accordingly, as shown in Figure 2B, the FA/Cu-resistance phenotype of CFR17, with its three copies of the CNV reporter, was noticeably stronger than that of CFR20 with two copies. It is unclear whether the

Table 1 Summary of the karyotype changes associated with the CNV reporter in the CFR clones.

	Haploids		Diploids		
	WT	*msh2Δ*	*WT*	*msh2Δ*	*ymrcty1-5Δ*
CFR clones isolated	26	22	29	22	16
Positive CFR upon retest	24	21	26	21	10
Karyotype changes					
Chr5 segmental duplication[a]	22	5	5	2	0
Chr13/chr5 translocation[b]	0	0	20	8	3
Chr7/chr5 translocation	0	0	0	0	5
Chr5 isochromosome[c]	0	0	0	0	1
Chr5 aneuploidy[d]	0	0	0	0	1
No karyotype change	2	16	1	11	0
CFR clones with CGH data	9	5	9	10	10

[a] Longer than normal chr5 molecules harboring tandem duplications or triplications of a segment of chr5 containing the CNV reporter flanked by direct repetitive full-length Ty1 or solo δ LTR elements.

[b] CFR511, a clone derived from the *ymrcty1-5Δ* homozygous diploid (JAY510), had a complex rearrangement consisting of a deletion of the right arm of chr13 from *YMRCTy1-4* to the right telomere, joined by a segment of chr5 containing a quadruplication of the segment containing the CNV reporter between *YERCTy1-1* and *YERCδ26*, in addition to one copy of the terminal segment between *YERCδ26* and *TEL05R*.

[c] CFR510, a clone derived from the *ymrcty1-5Δ* homozygous diploid (JAY510), had an isochromosome 5 formed by loss of the left arm from *TEL05L* to the Watson Ty1 element inserted at the *ura3-52* allele, joined by the segment from right arm from *YERCTy1-1* to *TEL05R*. This isochromosome was present in addition to the two parental size copies of chr5, both of which were retained in CFR510.

[d] CFR512, a clone derived from the *ymrcty1-5Δ* homozygous diploid (JAY510), had three copies of the parental size chr5, a simple aneuploidy of chr5.

triplication events occurred prior to the initial FA/Cu selection plating, or if they arose initially in cells carrying a duplication that then underwent a secondary NAHR event during the growth of the colony to expand to the 3× level. Since 3× cells are hyperresistant to FA/Cu, they would be expected to rapidly outnumber the 2× parent cells in the colony. It is also possible that such secondary rearrangements could be further stimulated by the growth in media containing FA, a known genotoxic agent (Kumari *et al.* 2012).

The phenotypic difference between the 2× and 3× reporter dosage levels in haploid strains, as well as our optimization trials, encouraged us to attempt the selection of spontaneous amplification rearrangements in diploid strains homozygous for the chr5 reporter insertion. We isolated several independent WT diploid CFR clones in FA/Cu media, repurified them under nonselective conditions, and found that most retested positive for FA/Cu resistance (Figure 3A and Table 1). In analyzing the karyotype changes in these diploid clones, we found that 5 of 25 CFRs had one chr5 homolog containing Ty1-mediated segmental duplications that were essentially identical to those seen in haploids, in addition to one parental copy of chr5 (*e.g.*, CFR73 in Figure 3C and CFR85 in Figure S6).

The majority of the diploid CFR clones, however, had a class of rearrangements not observed in haploids: nonreciprocal translocations, exemplified by CFR82 (Figure 3, B and D). In this case, the two parental copies of chr5 were unchanged, but one of the copies of chr13 was rearranged by the loss of a 176-kb segment between *YMRCTy1-5* and the right telomere (*TEL13R*) and the addition of a 128 kb chr5 segment from *YERCTy1-1* to *TEL05R*, which included the CNV reporter insertion. *YMRCTy1-5* is a Crick-oriented full Ty1 retrotransposon insertion that is present in our strain background near the *tR(UCU)M1* tRNA gene (at SGD coordinate 748,219), but that is absent in the S288c *S. cerevisiae* reference genomic sequence. This chr13/chr5 translocation results in an ∼875-kb chromosome visible in PFGE, with an overall reduction in size of ∼48 kb relative to the parental chr13. The presence of one remaining parental copy of chr13 made the loss of the large chr13 segment viable in the diploids, while the amplified segment of chr5 was responsible for the third copy of the CNV reporter that conferred the FA/Cu-resistance phenotype. This type of event is also shown schematically in Figure 1D.

Surprisingly, 20 of 25 independent WT diploid CFRs had the same 875-kb translocation band as CFR82. We used array CGH to analyze genomic DNA from three other of these clones and found the same chr13 deletion and chr5 amplification pattern in all three. These results indicated that the 875-kb chr13/chr5 translocation was a recurrent NAHR event. The fact that no other reporter-associated translocations were observed in the WT diploids suggested that 875-kb event must occur spontaneously at a rate substantially higher than that of other possible ectopic recombination interactions.

In addition to the chromosomal rearrangements that were associated with amplification of the CNV reporter, in a few cases, we also observed unselected karyotype changes in other regions of the genome. These unselected events were observed only in diploids and are shown in Figure S1. They included three trisomies (chr1, chr3, chr16) and five chromosomal rearrangements, four segmental duplications (chr3, chr4, chr12, chr13), and one nonreciprocal translocation between the right arm of chr3 and the left arm of chr5 in clone CFR100. The breakpoints in all five unselected rearrangements occurred at full-length Ty or LTR repeats; therefore, they were similar in nature to the selected FA/Cu-resistant chr5 amplifications.

One or more extra copies of the *SFA1–CUP1* gene dosage reporter were detected in all but two haploid and one diploid CFR clones (CFR16, 42, and 77, respectively). These three exceptions retested positive in the selective plates, but did not show any detectable karyotype changes in PFGE. In addition, we examined CFR16 by array CGH and also did not detect any gene dosage changes. These results suggested the existence of a secondary mechanism of FA/Cu resistance. We later found that these clones had acquired dominant point mutations in the *SFA1* gene. These mutations are presented at the end of the *Results* section.

Investigation of mechanisms for the recurrent chr13/chr5 translocation

We considered two hypotheses to explain the recurrence of the 875-kb translocation. The first was that *YMRCTy1-5* might be more similar in sequence to *YERCTy1-1* than any

other Ty element in the genome. Since the *YMRCTy1-5* sequence was not available in the reference genome, we PCR amplified and fully sequenced this element from our strain. We then constructed a sequence alignment containing *YERCTy1-1*, *YMRCTy1-5*, and the other 30 existing full-length Ty1 element sequences in the S288c reference genome (Figure S4). The alignments showed that *YMRCTy1-5* was indeed among the most similar Ty1 elements to *YERCTy1-1* (99.6% identity; with a 2981-bp segment of perfect homology). Nonetheless, we did find three other Ty1 elements (*YMLWTy1-2*, *YLRCTy1-1*, and *YPLWTy1-1*) that had even higher identity and had the same orientation with respect to the centromere as *YERCTy1-1*. These elements should in principle be competent to participate in NAHR with *YERCTy1-1* to generate other stable chromosomal translocations.

One function of the DNA mismatch repair system is to reduce the frequency of recombination between repeated genes that have sequence differences (Harfe and Jinks-Robertson 2000; George and Alani 2012). If near perfect sequence identity was important in affecting the recombination partners of *YERCTy1-1*, then by removing the DNA mismatch repair system we might be able to relax this constraint and observe translocations involving diverged Ty1 sequences from other chromosomes. We therefore tested haploid and diploid derivatives with a deletion of the *MSH2* gene, which is required for all functions of the mismatch repair system, including antirecombination activity (Surtees *et al.* 2004). We recovered 44 *msh2Δ* and *msh2Δ/msh2Δ* CFRs and examined their karyotypes by PFGE and array CGH. Only two classes of rearrangements were found in these mutants, and they were the same seen in the WT strains: chr5 segmental duplications and chr13/chr5 translocations. This result, coupled with the existence of other suitable Ty1 elements in the genome (>99% identity to *YERCTy1-1*), ruled out the recurrence of the chr13/chr5 translocation due to a sequence identity mechanism. However, one of the *msh2Δ/msh2Δ* clones (CFR99) had a chr13/chr5 translocation chromosome that was slightly larger than the others in its class (~895 kb *vs.* 875 kb), and had a chr13 array-CGH deletion breakpoint at *YMRWdelta19*, a solo LTR element positioned 20.6 kb distal to *YMRCTy1-5* (File S1 and Figure S5). The amplified region from chr5 was the same as in the other translocations, but the recombination event likely involved *YERWdelta20B*, which is in the compatible orientation to generate a stable monosomic rearrangement.

Even though there were no major qualitative differences in the chromosomal rearrangements found in the mismatch repair-deficient CFRs, we did find a substantial shift in their abundance relative to the number of clones without any detectable PFGE or array-CGH changes (*e.g.*, CFR93, Figure S6). Clones with normal karyotypes accounted for ~65% of all *msh2Δ* and *msh2Δ/msh2Δ* CFRs, suggesting the prevalence of a nucleotide mutation FA/Cu-resistance mechanism, rather than CNV (Table 1 and discussed below).

The second possibility we considered to explain the recurrence of chr13/chr5 875-kb translocation was the presence of a putative fragile site on the right arm chr13 located near the right telomere. By this explanation, *YMRCTy1-5* would not be actively responsible for this translocation, but instead, it would simply be the predominant site of repair of the precursor DSB associated with this fragile site. This scenario is plausible because *YMRCTy1-5* is the most distal full-length Ty1 element on the right arm of chr13 and, therefore, the first large NAHR substrate available to repair a DSB being resected from the right end of the chromosome. This explanation was also consistent with the observation of the CFR99 clone (Figure S5), which, possibly due to a relaxed sequence identity requirement in *msh2Δ/msh2Δ*, was repaired at an LTR repeat located distal (SGD coordinate 768,548) to the larger homology at *YMRCTy1-5*.

To test the fragile site hypothesis, we generated isogenic diploids with homozygous deletions of *YMRCTy1-5*. In this strain, DNA lesions formed at distal positions on the right arm and resected toward the centromere would no longer find a suitable recombination substrate, preventing the formation of the 875-kb chr13/chr5 translocation seen in WT cells. We analyzed the karyotypes of 10 independent CFRs derived from this strain and observed that the pattern of genome rearrangements had changed (Table 1). Remarkably, three of these CFRs still displayed deletions on the right arm of chr13, but the breakpoint in all three was at *YMRCTy1-4* (*e.g.*, CFR502, Figure 4C) located near SGD coordinate 375,000. In the absence of *YMRCTy1-5*, *YMRCTy1-4* became the first available full-length Ty1 NAHR substrate for repair of a lesion being resected from the right. Assuming that such lesion originated at a putative fragile site distal to *YMRCTy1-5*, this resection would have to span at least an additional 370 kb to reach *YMRCTy1-4*. Chromosomal rearrangements that involve long-range processing of a distally located DSB up to a Ty element have also been observed previously (Hoang *et al.* 2010).

Another interesting observation in the strain with the deletion of *YMRCTy1-5* was the appearance of a different recurrent rearrangement. Five of 10 CFRs had the same 925-kb chr7/chr5 translocation that comigrated with chr16 and chr13 in PFGE (*e.g.*, CFR501; Figure 4A). This translocation was composed of a deletion of chr7 right arm sequences distal to *YGRCTy1-3* and amplification of chr5 sequences from *YERCTy1-1* to the right telomere (Figure 4B). In addition, we observed one strain that was trisomic for chr5 and one strain with a chr5/chr5 translocation (isochromosome) involving *YERCTy1-1* and the Watson-oriented Ty1 element inserted at the *ura3-52* allele on the left arm.

One explanation for the changes observed in the CNV spectrum in the *ymrcty1-5Δ/ymrcty1-5Δ* diploids was that the extensive resection required for ectopic repair of the distal DNA lesion lowered the recovery of CFRs with chr13 deletions. This lengthier and more time-consuming resection would provide additional opportunities for allelic repair

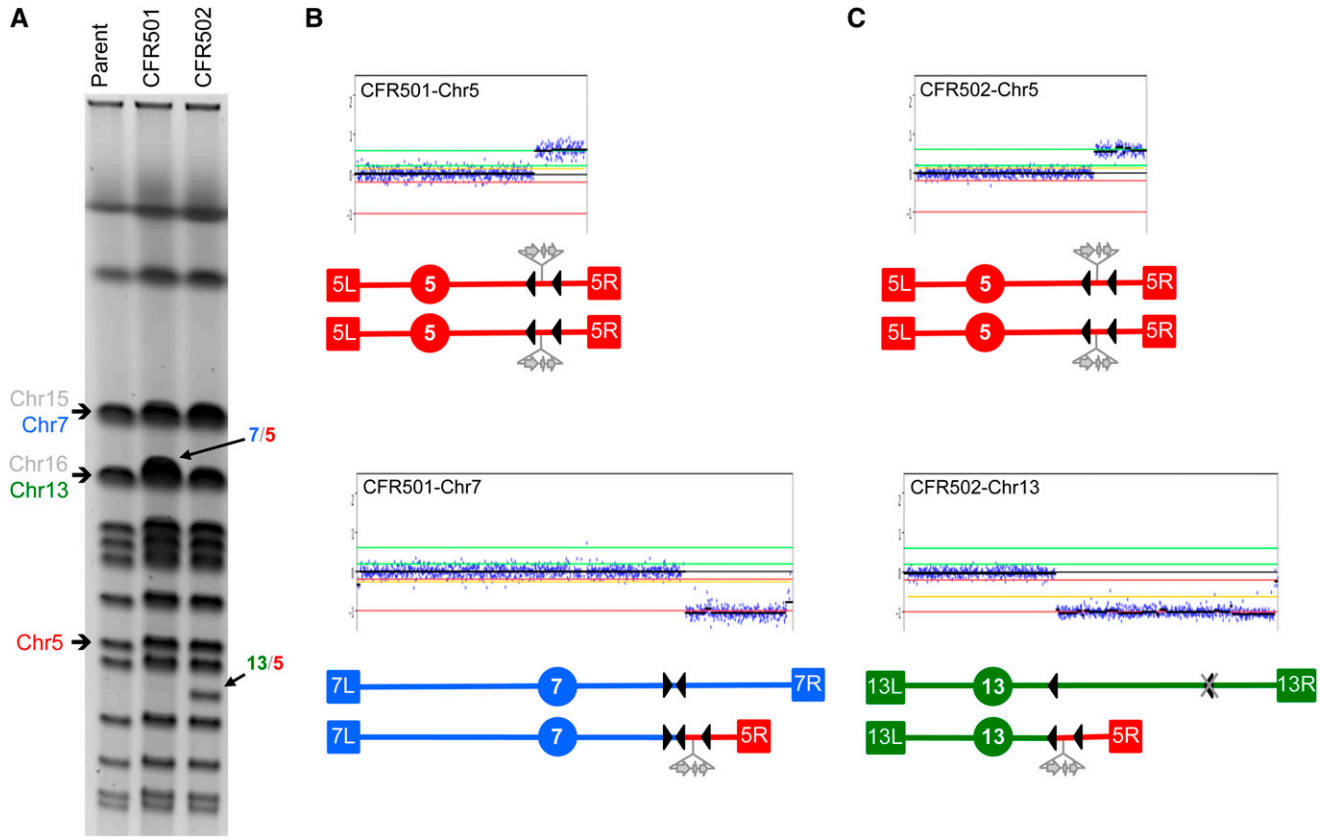

Figure 4 Alternative translocations in diploids lacking the *YMRCTy1-5* repeat element. Schematic representations are as in Figure 2. Chr5 is shown in red, chr13 is shown in green, and chr7 is shown in blue. (A) PFGE showing the karyotypes of parent diploid strain JAY510 and of derivative clones CFR501 (containing a chr7/chr5 translocation) and CFR502 (containing a chr13/chr5 translocation). The parental bands for chr5, chr7, and chr13 involved in the rearrangements are indicated to the left; also indicated are chr16 and chr15, which comigrate with chr13 and chr7, respectively. (B) Array-CGH plots and schematic representation of chr5 and chr7 in the CFR501 clone. The breakpoints correspond to *YERCTy1-1* in chr5 and *YGRWTy2-2/YGRCTy1-3* in chr7. (C) Array-CGH plots and schematic representation of chr5 and chr13 in the CFR502 clone. The breakpoints correspond to *YERCTy1-1* in chr5 and *YMRCTy1-4* in chr13. Note the deletion of the *YMRCTy1-5* element in this strain, represented by the gray X over the normal position of this element (distal/right arrowhead).

of the DSB using the intact sister chromatid or homolog, an outcome that is not detectable in the CNV assay. As a consequence, other less-abundant NAHR events became more prevalent among the FA/Cu-resistant clones. The results obtained with the *ymrcty1-5Δ/ymrcty1-5Δ* diploids also uncovered the existence of a second recurrent translocation event, involving the right arm of chr7.

Supporting evidence and initial mapping of a candidate chr13 right arm fragile site

The results of the CNV assays described above suggested the existence of a frequent DNA lesion on the right end of chr13, responsible for triggering the recurrent translocations observed in the diploid CFRs. To obtain independent support for this possibility, we generated a hybrid diploid strain marked to allow the detection of LOH events on chr13. Allelic recombination repair is a much more frequent event than NAHR; however, because our diploid CNV strain is isogenic, it was not suitable to detect LOH. We therefore crossed our haploid strain to a haploid isogenic with YJM789, a highly diverged strain background (Wei *et al.* 2007). The resulting hybrid diploid has a large number of heterozygous single-nucleotide polymorphisms (SNPs) that can be followed to analyze recombination on a genome-wide basis (Lee *et al.* 2009). In addition to the SNPs, we inserted a *URA3–Kan* cassette on the CG379-derived homolog of chr13, downstream of the *ADH6* gene about 10 kb from the right telomere (Figure 5A). A DSB formed in the CG379 homolog and repaired through allelic recombination with the YJM789 homolog may result in LOH of the markers between the site of recombination repair and the right telomere, including the loss of the *URA3* marker. The presumption in this experiment was that a discrete fragile site in this region would produce a bias in the distribution of sites of LOH recombination, causing an excess of breakpoints to be detected in its vicinity (Tang *et al.* 2011).

Independent spontaneous LOH events were selected in plates containing 5-FOA, and the rate of these events was determined to be 2.4×10^{-5} LOH events/cell division (95% confidence interval: $1.7–3.9 \times 10^{-5}$). We then analyzed 12 FOA^R clones using custom allele-specific microarrays to determine their genome-wide SNP genotype (CG379, YJM789,

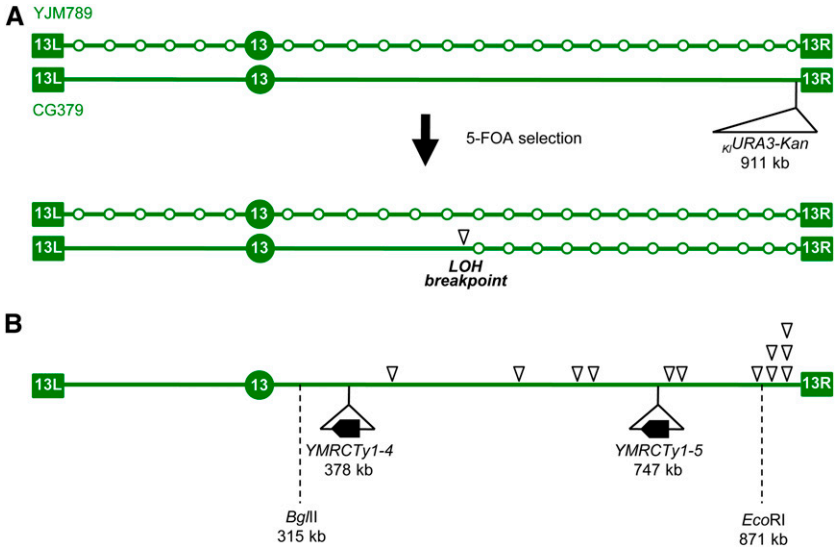

Figure 5 Initial mapping of a candidate fragile site on the right arm of chr13. (A) Experimental rationale. Schematic representation of chr13 in the hybrid diploid strain (JAY800 and JAY801), formed by mating haploids of the diverged strain backgrounds YJM789 and CG379. The open circles in the YJM789-derived chromosome represent SNP positions. The *KIURA3-Kan* marker was inserted in the CG379-derived chromosome, downstream of the *ADH6* gene, near the right telomere. Mitotic crossovers initiated by DNA breaks in the CG379-derived chromosome and repaired using the YJM789 homolog as template result in clones that are resistant to 5-FOA and homozygous for the right end of the YJM789-derived chr13. Genotyping with SNP microarrays can determine the precise site of allelic mitotic recombination (LOH breakpoint, open arrowhead). This site should occur in close proximity to the precursor DNA lesion. (B) LOH breakpoint positions for 12 independent 5-FOA-resistant clones determined by SNP microarray genotyping showing a clustering of breakpoints near the right end of chr13. Also indicated are the relative positions of the two Ty1 elements involved in the chr13/chr5 translocations described in Figures 3 and 4 and the position of the SNP–RFLP markers *Bgl*II and *Eco*RI. The *Eco*RI marker is described in the *Results*. The genotype at *Bgl*II marker site was also determined and found to be heterozygous in most 5-FOA^R clones (117/131; 89.3%).

or heterozygous) (St Charles *et al.* 2012). As expected from the 5-FOA selection, all 12 clones analyzed displayed terminal LOH on the right arm of chr13. Fifty percent of the detected LOH breakpoints (inverted triangles in Figure 5B) were found in the 41-kb region immediately proximal to the *URA3–Kan* insertion site, which corresponded to only 6.3% of the possible recombination window (distance *CEN13 to URA3-Kan* = 643 kb). The other half of the 5-FOA^R clones had breakpoints scattered through the rest of the right arm.

Since the pattern observed in the SNP microarray experiment was suggestive of a bias in the distribution of LOH breakpoints, we examined a larger number of FOA^R clones to assess the significance of this find. We genotyped these additional clones for a SNP marker 40 kb proximal to *URA3–Kan*. This SNP was located at the approximate boundary of the breakpoint cluster detected by microarrays and corresponded to an *Eco*RI restriction site (SGD chr13 coordinate 870,864) in the CG379 homolog that was absent in the YJM789 homolog. Using primers that flanked the polymorphism, we generated a PCR fragment for 130 independent 5-FOA^R diploids, treated the fragments with *Eco*RI, and examined the products by gel electrophoresis. Of the 130 new LOH clones, 109 were homozygous for the YJM789 SNP, 20 were heterozygous, and 1 was homozygous for the CG379 SNP (possibly within a mitotic gene conversion tract associated with LOH). Therefore, 21 of 130 clones had an LOH breakpoint distal to the *Eco*RI site. Based on the size of this interval relative to the distance between *CEN13* and the *URA3–Kan* insertion, we expect only eight events. By chi-square analysis, this difference is very significant ($P = 2.8 \times 10^{-6}$). This deviation was even more pronounced when we considered the PCR–RFLP and microarray data together ($P = 2.5 \times 10^{-9}$). We interpret these results as evidence for the presence of a frequent recombination-initiating lesion near the right end of chr13, perhaps a DSB formed at a chromosomal fragile site. Alternatively, it is possible that the right telomere of chr13 is poorly maintained and frequently becomes "uncapped," allowing resection beginning at the telomere itself and extending into telomere-proximal chromosome sequences.

Characterization of new SFA1 dominant alleles

As discussed above, we detected CFR clones that retested positive for the FA/Cu-resistance phenotype but did not have any detectable chromosomal rearrangements. This class was particularly abundant in the mismatch-repair deficient strains suggesting a nucleotide mutation-based mechanism of resistance. In addition, because we identified several such isolates from diploid strains, these point mutations would have to be dominant/gain-of-function alterations to display the resistance phenotype in the presence of the second wild-type allele.

To characterize this possible mutation, we first crossed two *msh2Δ* haploid CFR isolates from this class (CFR49 and CFR50, *MAT*α) to a wild-type strain (JAY377, *MAT*a). All three haploid strains had only one copy of the CNV reporter, but CFR49 and CFR50 had the *Kan* G418 resistance marker linked to the reporter, whereas JAY377 had the *Hph* hygromycin B resistance marker at the same position (Figure 2A). We tested the corresponding diploids for FA/Cu resistance. Both diploids derived were FA/Cu resistant, confirming that the mutations in the two CFR clones were dominant (Figure 6A). Next, we sporulated and dissected tetrads from these diploids to examine the segregation pattern of the resistance phenotype. We observed two resistant and two sensitive spores, indicating that the mutant phenotype was controlled by only one locus. In addition, we also scored the spores for the *Kan* and *Hph* markers associated with CNV reporter. As expected, both markers segregated 2:2, and spores were

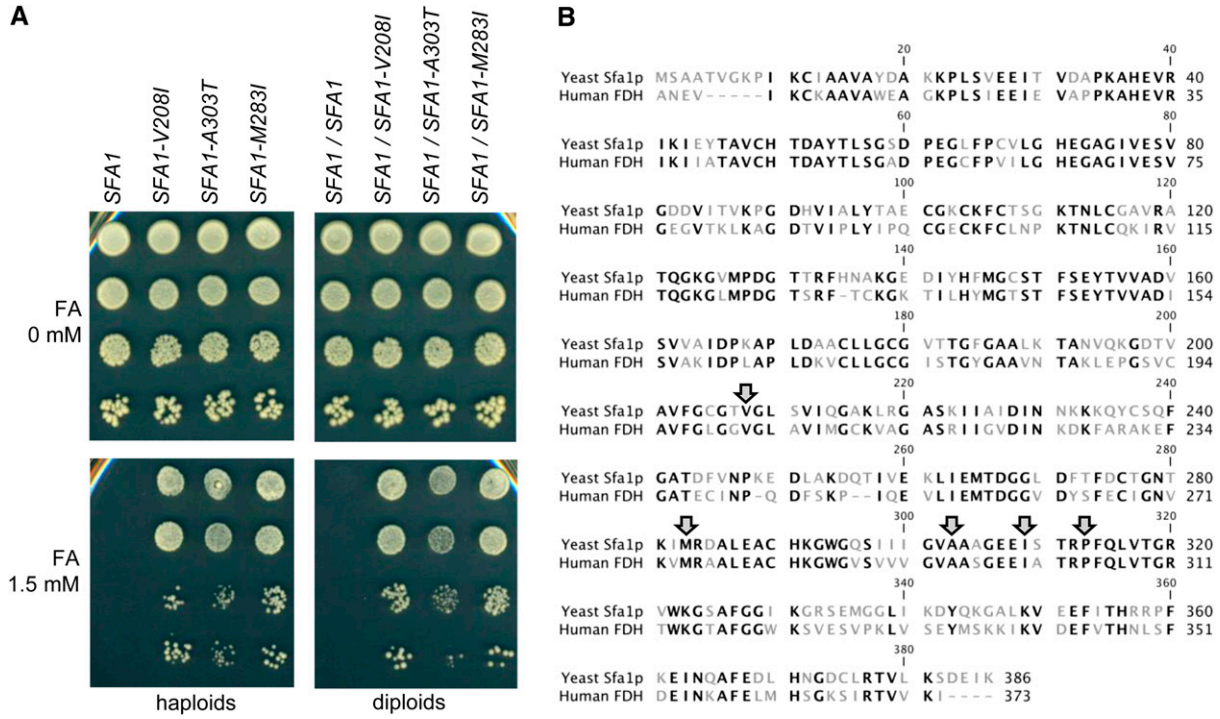

Figure 6 Characterization of dominant mutant alleles of the *SFA1* gene. (A) Formaldehyde (FA)-resistance phenotype in haploid (left) and heterozygous diploid (right) strains carrying three different mutant alleles of *SFA1*. The genotypes are indicated at the top. Serial dilutions were plated in media containing 0 or 1.5 mM FA as indicated to the left. No $CuSO_4$ was added. (B) Amino acid residue sequence alignment between the *S. cerevisiae* Sfa1p and the human FDH enzymes. Conserved residues (60.9% identity) are shown in black letters, and diverged residues are shown in gray. Shaded arrows point to the five residues that were substituted in the dominant *SFA1* mutations.

either $G418^R$ Hyg^S or $G418^S$ Hyg^R. However, we noted that FA/Cu resistance always cosegregated with G418 resistance. Since both CFR49 and CFR50 had CNV reporters marked with *Kan*, this result indicated that their FA/Cu-resistance mutations were tightly linked to the CNV reporter, presumably in the *SFA1* or *CUP1* genes.

We then PCR amplified and sequenced the CNV reporter from 13 independent CNV-less CFRs to find the nucleotide mutations. This analysis showed that all sequenced clones carried mutations in the *SFA1* gene. Since the mutations were in *SFA1*, we repeated the resistance assays in plates containing FA or Cu separately. This analysis showed that the *SFA1* mutations did not alter resistance to Cu (data not shown) and that their effect on resistance to FA was quite pronounced (Figure 6A). In fact, a single copy of the mutant *SFA1* alleles conferred a level of FA resistance comparable to that seen in a strain carrying three copies of the wild-type *SFA1* gene (data not shown).

A total of five different dominant *SFA1* alleles were identified. Two of the alleles arose independently multiple times: *SFA1–Val208Ile* (nucleotide mutation G622A) occurred in nine cases, and *SFA1–Ala303Thr* (nucleotide mutation G907A) occurred three times. Alleles *SFA1–Met283Ile*, *SFA1–Ile309Met*, and *SFA1–Pro313Ala* occurred once each. All alleles sequenced were isolated from *msh2Δ* haploids, except for *SFA1–Met283Ile*, which was isolated in a *MSH2* haploid (CFR16).

To gain insight into the potential effect of these mutations on the enzymatic activity of Sfa1p, we analyzed them in the context of the human glutathione-dependent formaldehyde dehydrogenase enzyme (hFDH) for which a crystal structure has been solved (Sanghani *et al.* 2002a,b). All five dominant alleles corresponded to residues that are conserved between the human and yeast enzymes (Figure 6B). Interestingly, the two alleles most frequently isolated (*SFA1–Val208Ile* and *SFA1–Ala303Thr*) are located in the active site of hFDH, in direct contact with the NAD(P)+ coenzyme. This structural arrangement raises the possibility that mutation at these specific residues may destabilize the binding of the coenzyme, facilitating its release from the active site after the reaction with the *S*-hydromethylglutathione. This would accelerate the rate at which FA is detoxified, therefore enhancing FA resistance without increasing the number of copies of the *SFA1* gene.

Discussion

A new assay for copy-number variation

In this study, we took advantage of the gene dosage-dependent phenotypes of the *SFA1* and *CUP1* genes to develop an optimized assay for the detection of gene amplifications. While several analogous systems have been previously reported in yeast, few of them have the sensitivity

necessary to select low-order amplification events. In contrast, our system is capable of identifying spontaneous chromosomal rearrangements, resulting in a simple doubling of the region of interest, going from one to two copies, and also subtler (50%) increases in gene dosage, going from two to three copies. This sensitivity makes the system equally suited for the analysis of amplifications in haploid and diploid cells, whereas most previous systems function exclusively in haploids. We believe our system is an attractive and more germane model for the somatic CNVs commonly observed in humans (Frohling and Dohner 2008; Girirajan *et al.* 2011) and represents a valuable new tool for the investigation of structural genomic variation in a biomedically relevant context.

Another distinctive quality of this assay is that it allows the detection of chromosomal rearrangements initiated by rare spontaneous DNA lesions, regardless of where in the genome they occur. These lesions may include not only DSBs, but also uncapped telomeres, collapsed replication intermediates that switch DNA template, or any other recombination-initiating event. For example, in the case of the translocations detected in diploids, the precursor lesions likely occurred on chr13 or on chr7, but the CNV reporter was inserted on chr5. Conventional assays that are based on deletions such as DEL or GCR (Schiestl 1989; Chen and Kolodner 1999), or amplification assays using haploids (Payen *et al.* 2008), are thought to detect rearrangements initiated predominantly by lesions in the immediate vicinity of their respective reporter sequences. The same issue is even more pronounced in assays that rely on the induction of site-specific DSBs (*e.g.*, *HO*, I-*Sce*I endonucleases) to raise the frequency of recombination up to a high level required for detection. The spontaneous and genome-wide nature of the FA/Cu-resistance assay is a highly desirable feature because, in principle, it should provide experimental results that more broadly represent global genomic instability processes, rather than the local properties of specific loci that may not necessarily apply to other regions.

The versatility of this detection system allowed us to conduct parallel genome stability experiments in the same chromosomal context in haploids and diploids. We observed that the classes of chromosomal rearrangements associated with each ploidy state were quite specific and distinct. In haploids we identified only segmental duplications and, as expected, no associated large deletions. Segmental duplications were generally also observed in most other previously reported haploid genome rearrangement assays, with the notable exception of the translocations detected in the recent iterations of the GCR assay, in which a deletion of the relatively small and nonessential terminal region of chr5 left arm is associated with the duplication of a terminal segment from a different chromosome (Putnam *et al.* 2009; Chan and Kolodner 2011, 2012). The diploid CFR clones displayed two main classes of rearrangements: ~15% were segmental duplications similar to those found in the haploids, but most others were nonreciprocal translocations resulting in amplification of the right arm of chr5 (including the CNV reporter) coupled with a deletion of a terminal segment of a different chromosome. We also detected a clone (CFR512) containing a trisomy of chr5, and incidentally, this same clone also carried two unselected trisomies of chr3 and chr16. These and other unselected karyotype changes were observed only in diploid clones. In summary, these data confirmed that diploid cells can tolerate a more diverse repertory of rearrangements than haploids and therefore provide a richer platform to study genome stability.

Another key observation was that all chromosomal rearrangement breakpoints detected in this study contained dispersed repetitive DNA sequences, either full-length Ty or solo LTR elements. No breakpoints were detected at single-copy or microhomology sequences. This pattern was consistent with several other studies that implicated Ty sequences as hotspots for chromosomal rearrangements (Mieczkowski *et al.* 2006; Scheifele *et al.* 2009) and confirmed that NAHR is the primary DSB repair pathway responsible for such events in yeast. Interestingly, the spontaneous rearrangements selected in the CFR diploid clones were reminiscent of those we found in isogenic, G2-synchronized diploids that survived exposure to 800 Gy of ionizing radiation resulting in ~250 DSBs per cell (Argueso *et al.* 2008). The NAHR-mediated segmental duplications and translocations identified in that high-dose γ-ray experiment were qualitatively indistinguishable from the ones selected spontaneously in this study. The only meaningful difference was the massive drop in the overall frequency of occurrence: two to three rearrangements per 800 Gy surviving cell, compared to one rearrangement per approximately 10^6 viable cells at the 0-Gy dose. This suggests that the FA/Cu-resistance assay may be successfully used to study CNV formation following low doses of radiation, as well as other clastogenic environmental exposures.

Dominant formaldehyde hyperresistant alleles of SFA1

During the course of our study, we unexpectedly identified dominant mutations in the *SFA1* gene that increased the resistance of cells to formaldehyde, presumably through increased activity of the formaldehyde dehydrogenase (FDH) enzyme. This was intriguing and unusual, since mutations that result in the substitution of conserved amino acid residues at the core of an enzyme's active site are often associated with reduction or complete loss of activity and are typically recessive. This result also suggests that the natural selection forces that have acted on the sequence of *SFA1* stopped short of the maximum possible biochemical activity, therefore implying that a super-active FDH may somehow be associated with negative fitness consequences. Regardless of the their role in the evolution of *SFA1*, the fact that the mutations have significantly increased activity, and consequently a larger FA-resistance phenotypic differential between one and two mutant copies, provided an opportunity for the improvement of this gene as a reporter for gene dosage. Recent work in our laboratories using the *SFA1* mutant

alleles in the CNV reporter showed a pronounced reduction in background colony growth when cultures were plated at high cell densities (to be presented elsewhere), in effect enabling future versions of the CNV assay that will be fully quantitative.

Detection of recurrent chromosomal rearrangements

Our analysis of spontaneous amplifications selected from diploid clones revealed a remarkable recurrence of a specific chromosomal rearrangement between the right arms of chr13 and chr5. We took two experimental approaches to address this result. First, we created a derivative strain deleted for a central component of the DNA mismatch repair system (*msh2Δ/msh2Δ*) that should relax sequence identity constraints imposed on recombination partner choice (George and Alani 2012). This strain produced the very same rearrangements as the wild type, indicating that sequence similarity is not an important factor driving the recurrence of this translocation.

The second factor we investigated was the possible presence of a chromosomal fragile site on the right arm of chr13. Previous studies from our group and others have shown that frequent breaks are associated with certain Ty sequences under conditions of replication stress and that these breaks can be potent inducers of chromosomal rearrangements (Cha and Kleckner 2002; Lemoine *et al.* 2005). Replication stress is a well-characterized activator of fragile site expression in humans (Arlt *et al.* 2012). However, it is important to note that the fragile nature may not be entirely dependent on replication stress. For example, the same yeast fragile sites have also been detected as hotspots for NAHR even under normal growth conditions (Hoang *et al.* 2010; Chan and Kolodner 2012).

We tested the candidate chr13R fragile site in two ways. We deleted the *YMRCTy1-5* element and observed that in some cases the rearrangements recovered involved a proximal Ty element on the right arm of chr13. We then examined spontaneous allelic recombination clones containing LOH on the right arm of chr13 and found a statistically significant clustering of breakpoints consistent with the presence of a candidate fragile site in the region. Taken together, these results suggested the possibility of a frequent DSB distal to the *YMRCTy1-5* element, which could be the trigger for the recurrent chr13/chr5 translocations. Alternatively, a telomere with a partial defect in capping might also account for the high incidence of chr13R rearrangements.

In either the fragile site or weak telomere scenarios, a region of chr13 at least ~150 kb would have to be resected to expose the homology at *YMRCTy1-5* and initiate NAHR. Chromosomal rearrangements involving similarly long resection tracts (break-distal recombination, BDR) have been recently reported (Hoang *et al.* 2010; Tan *et al.* 2012). While the DSB at chr13R explanation is attractive, it is unlikely to be the only factor involved. Several other Ty repeats exist in the genome that should in principle be competent to participate in translocations, yet none of those other sites were detected with the wild-type diploid strain. This suggests that there may be other significant contributing cellular mechanisms.

We considered three other factors that may be favoring the detection of this specific NAHR interaction in the FA/Cu-resistance assay. The first is not related to a recombination mechanism, but rather may be associated with the viability of clones. This would be possible if cells carrying the chr13/chr5 translocation somehow had higher FA/Cu resistance and would therefore form colonies more often than cells with other rearrangements. We do not think this is the case for two reasons. We compared the relative viability and growth of clones carrying the chr13/chr5 rearrangements with clones carrying the chr7/chr5 translocation or the chr5 SDs in media containing FA/Cu (data not shown). These three classes of clones appeared to be just as viable between them. In addition, even if chr13/chr5 translocation had a more robust growth, this would not prevent the recovery of other, less robust rearrangements that should also be viable in diploid cells.

Another factor that could create the observed detection bias is the relative proximity between potential recombination partner sequences in the tridimensional structure of the genome. This mechanism has been invoked as a contributor to the formation of recurrent chromosomal rearrangements in cancer cells (Wijchers and de Laat 2011). Thus, we analyzed the available structure of the *S. cerevisiae* genome (Duan *et al.* 2010) and asked whether proximity between the right arms of chr5 and chr13 might explain the observed rearrangements. This analysis showed that the reverse is true: these two chromosomes are relatively farther apart from each other than from other chromosomes. This observation suggests that the relative position of a sequence in the static model of the genome may not be as important for recombination as its ability to move around the nucleus during DSB repair. Two recent studies have elegantly demonstrated that yeast DNA sequences undergo a rapid transition from a relatively constrained nuclear localization to an increased mobility state immediately after a nearby DSB is induced (Dion *et al.* 2012; Mine-Hattab and Rothstein 2012). According to this model, a lesion on chr13 would engage the chr5 donor sequence not because of static proximity, but rather through a higher-than-normal degree of freedom to explore the nuclear space in search for homology. It would be interesting to investigate if the newly discovered transition from static to mobile status varies between different regions of the genome and whether some sequences are able to explore larger nuclear volumes than others following breakage.

Finally, we note that a recent haploid yeast study also identified recurrent nonreciprocal translocations involving dispersed Ty1 elements (Chan and Kolodner 2012). In that study, six Ty1 elements (including *YERCTy1-1*) were used as donor sequences repeatedly (~70% of cases) at frequencies much higher than those expected from random choice. As was the case in our analysis, the authors did not find

a significant correlation between the relative spatial proximity in nucleus of the recombining elements or their degree of nucleotide sequence similarity. However, their results and our own clearly showed that strong, yet unknown, mechanisms exist in the yeast nucleus that drive specific Ty repeats toward preferential NAHR with others. Understanding these processes could shed some much needed light into the origins of recurrent chromosomal rearrangements in cancer cells.

Acknowledgments

We thank Thomas Hurley for helpful discussions on the modeling on the *SFA1* dominant mutations onto the crystal structure of the hFDH enzyme. The CNV research in the Petes, Argueso, and Mieczkowski laboratories was supported by an American Recovery and Reinvestment Act National Institutes of Health (NIH)–National Institute of Environmental Health Sciences Challenge Grant (5RC1ES018091-02). In addition, T.D.P. was supported by NIH grants GM24110 and GM52319, and J.L.A. was supported by American Cancer Society grant ACS IRG no. 57-001-53.

Literature Cited

Abrahams, B. S., and D. H. Geschwind, 2008 Advances in autism genetics: on the threshold of a new neurobiology. Nat. Rev. Genet. 9: 341–355.

Argueso, J. L., J. Westmoreland, P. A. Mieczkowski, M. Gawel, T. D. Petes *et al.*, 2008 Double-strand breaks associated with repetitive DNA can reshape the genome. Proc. Natl. Acad. Sci. USA 105: 11845–11850.

Arlt, M. F., T. E. Wilson, and T. W. Glover, 2012 Replication stress and mechanisms of CNV formation. Curr. Opin. Genet. Dev. 22: 204–210.

Brewer, B. J., C. Payen, M. K. Raghuraman, and M. J. Dunham, 2011 Origin-dependent inverted-repeat amplification: a replication-based model for generating palindromic amplicons. PLoS Genet. 7: e1002016.

Brown, C. J., K. M. Todd, and R. F. Rosenzweig, 1998 Multiple duplications of yeast hexose transport genes in response to selection in a glucose-limited environment. Mol. Biol. Evol. 15: 931–942.

Cha, R. S., and N. Kleckner, 2002 ATR homolog Mec1 promotes fork progression, thus averting breaks in replication slow zones. Science 297: 602–606.

Chan, J. E., and R. D. Kolodner, 2011 A genetic and structural study of genome rearrangements mediated by high copy repeat Ty1 elements. PLoS Genet. 7: e1002089.

Chan, J. E., and R. D. Kolodner, 2012 Rapid analysis of *Saccharomyces cerevisiae* genome rearrangements by multiplex ligation-dependent probe amplification. PLoS Genet. 8: e1002539.

Chen, C., and R. D. Kolodner, 1999 Gross chromosomal rearrangements in *Saccharomyces cerevisiae* replication and recombination defective mutants. Nat. Genet. 23: 81–85.

Cheng, E., J. A. Vaisica, J. Ou, A. Baryshnikova, Y. Lu *et al.*, 2012 Genome rearrangements caused by depletion of essential DNA replication proteins in *Saccharomyces cerevisiae*. Genetics 192: 147–160.

Dion, V., V. Kalck, C. Horigome, B. D. Towbin, and S. M. Gasser, 2012 Increased mobility of double-strand breaks requires Mec1, Rad9 and the homologous recombination machinery. Nat. Cell Biol. 14: 502–509.

Dorsey, M., C. Peterson, K. Bray, and C. E. Paquin, 1992 Spontaneous amplification of the *ADH4* gene in *Saccharomyces cerevisiae*. Genetics 132: 943–950.

Duan, Z., M. Andronescu, K. Schutz, S. McIlwain, Y. J. Kim *et al.*, 2010 A three-dimensional model of the yeast genome. Nature 465: 363–367.

Dunham, M. J., H. Badrane, T. Ferea, J. Adams, P. O. Brown *et al.*, 2002 Characteristic genome rearrangements in experimental evolution of *Saccharomyces cerevisiae*. Proc. Natl. Acad. Sci. USA 99: 16144–16149.

Erhart, E., and C. P. Hollenberg, 1983 The presence of a defective *LEU2* gene on 2 mu DNA recombinant plasmids of *Saccharomyces cerevisiae* is responsible for curing and high copy number. J. Bacteriol. 156: 625–635.

Fink, G. R., and C. A. Styles, 1974 Gene conversion of deletions in the *his4* region of yeast. Genetics 77: 231–244.

Frohling, S., and H. Dohner, 2008 Chromosomal abnormalities in cancer. N. Engl. J. Med. 359: 722–734.

Gangloff, S., H. Zou, and R. Rothstein, 1996 Gene conversion plays the major role in controlling the stability of large tandem repeats in yeast. EMBO J. 15: 1715–1725.

George, C. M., and E. Alani, 2012 Multiple cellular mechanisms prevent chromosomal rearrangements involving repetitive DNA. Crit. Rev. Biochem. Mol. Biol. 47: 297–313.

Girirajan, S., C. D. Campbell, and E. E. Eichler, 2011 Human copy number variation and complex genetic disease. Annu. Rev. Genet. 45: 203–226.

Green, B. M., K. J. Finn, and J. J. Li, 2010 Loss of DNA replication control is a potent inducer of gene amplification. Science 329: 943–946.

Gresham, D., M. M. Desai, C. M. Tucker, H. T. Jenq, D. A. Pai *et al.*, 2008 The repertoire and dynamics of evolutionary adaptations to controlled nutrient-limited environments in yeast. PLoS Genet. 4: e1000303.

Hansche, P. E., V. Beres, and P. Lange, 1978 Gene duplication in *Saccharomyces cerevisiae*. Genetics 88: 673–687.

Harfe, B. D., and S. Jinks-Robertson, 2000 DNA mismatch repair and genetic instability. Annu. Rev. Genet. 34: 359–399.

Hastings, P. J., G. Ira, and J. R. Lupski, 2009 A microhomology-mediated break-induced replication model for the origin of human copy number variation. PLoS Genet. 5: e1000327.

Hawthorne, D. C., 1963 A deletion in yeast and its bearing on the structure of the mating type locus. Genetics 48: 1727–1729.

Herskowitz, I., 1988 The Hawthorne deletion twenty-five years later. Genetics 120: 857–861.

Hoang, M. L., F. J. Tan, D. C. Lai, S. E. Celniker, R. A. Hoskins *et al.*, 2010 Competitive repair by naturally dispersed repetitive DNA during non-allelic homologous recombination. PLoS Genet. 6: e1001228.

Iskow, R. C., O. Gokcumen, and C. Lee, 2012 Exploring the role of copy number variants in human adaptation. Trends Genet. 28: 245–257.

Itsara, A., H. Wu, J. D. Smith, D. A. Nickerson, I. Romieu *et al.*, 2010 De novo rates and selection of large copy number variation. Genome Res. 20: 1469–1481.

Kim, H. M., V. Narayanan, P. A. Mieczkowski, T. D. Petes, M. M. Krasilnikova *et al.*, 2008 Chromosome fragility at GAA tracts in yeast depends on repeat orientation and requires mismatch repair. EMBO J. 27: 2896–2906.

Koshland, D., J. C. Kent, and L. H. Hartwell, 1985 Genetic analysis of the mitotic transmission of minichromosomes. Cell 40: 393–403.

Koszul, R., S. Caburet, B. Dujon, and G. Fischer, 2004 Eucaryotic genome evolution through the spontaneous duplication of large chromosomal segments. EMBO J. 23: 234–243.

Krepischi, A. C., P. L. Pearson, and C. Rosenberg, 2012 Germline copy number variations and cancer predisposition. Future Oncol. 8: 441–450.

Kumari, A., Y. X. Lim, A. H. Newell, S. B. Olson, and A. K. McCullough, 2012 Formaldehyde-induced genome instability is suppressed by an XPF-dependent pathway. DNA Repair 11: 236–246.

Lea, D. E., and C. A. Coulson, 1949 The distribution of the numbers of mutants in bacterial populations. J. Genet. 28: 491–511.

Lee, P. S., P. W. Greenwell, M. Dominska, M. Gawel, M. Hamilton *et al.*, 2009 A fine-structure map of spontaneous mitotic crossovers in the yeast *Saccharomyces cerevisiae*. PLoS Genet. 5: e1000410.

Lemoine, F. J., N. P. Degtyareva, K. Lobachev, and T. D. Petes, 2005 Chromosomal translocations in yeast induced by low levels of DNA polymerase a model for chromosome fragile sites. Cell 120: 587–598.

Libuda, D. E., and F. Winston, 2006 Amplification of histone genes by circular chromosome formation in *Saccharomyces cerevisiae*. Nature 443: 1003–1007.

Liebman, S., P. Shalit, and S. Picologlou, 1981 Ty elements are involved in the formation of deletions in DEL1 strains of *Saccharomyces cerevisiae*. Cell 26: 401–409.

Liebman, S. W., A. Singh, and F. Sherman, 1979 A mutator affecting the region of the iso-1-cytochrome c gene in yeast. Genetics 92: 783–802.

Malhotra, D., and J. Sebat, 2012 CNVs: harbingers of a rare variant revolution in psychiatric genetics. Cell 148: 1223–1241.

McCulley, J. L., and T. D. Petes, 2010 Chromosome rearrangements and aneuploidy in yeast strains lacking both Tel1p and Mec1p reflect deficiencies in two different mechanisms. Proc. Natl. Acad. Sci. USA 107: 11465–11470.

Mieczkowski, P. A., F. J. Lemoine, and T. D. Petes, 2006 Recombination between retrotransposons as a source of chromosome rearrangements in the yeast *Saccharomyces cerevisiae*. DNA Repair 5: 1010–1020.

Mine-Hattab, J., and R. Rothstein, 2012 Increased chromosome mobility facilitates homology search during recombination. Nat. Cell Biol. 14: 510–517.

Moore, I. K., M. P. Martin, and C. E. Paquin, 2000 Telomere sequences at the novel joints of four independent amplifications in *Saccharomyces cerevisiae*. Environ. Mol. Mutagen. 36: 105–112.

Morrison, A., J. B. Bell, T. A. Kunkel, and A. Sugino, 1991 Eukaryotic DNA polymerase amino acid sequence required for 3′-5′ exonuclease activity. Proc. Natl. Acad. Sci. USA 88: 9473–9477.

Narayanan, V., P. A. Mieczkowski, H. M. Kim, T. D. Petes, and K. S. Lobachev, 2006 The pattern of gene amplification is determined by the chromosomal location of hairpin-capped breaks. Cell 125: 1283–1296.

Ozenberger, B. A., and G. S. Roeder, 1991 A unique pathway of double-strand break repair operates in tandemly repeated genes. Mol. Cell. Biol. 11: 1222–1231.

Paques, F., and J. E. Haber, 1999 Multiple pathways of recombination induced by double-strand breaks in *Saccharomyces cerevisiae*. Microbiol. Mol. Miol. Rev. 63: 349–404.

Payen, C., R. Koszul, B. Dujon, and G. Fischer, 2008 Segmental duplications arise from Pol32-dependent repair of broken forks through two alternative replication-based mechanisms. PLoS Genet. 4: e1000175.

Petes, T. D., 1980 Unequal meiotic recombination within tandem arrays of yeast ribosomal DNA genes. Cell 19: 765–774.

Putnam, C. D., V. Pennaneach, and R. D. Kolodner, 2005 *Saccharomyces cerevisiae* as a model system to define the chromosomal instability phenotype. Mol. Cell. Biol. 25: 7226–7238.

Putnam, C. D., T. K. Hayes, and R. D. Kolodner, 2009 Specific pathways prevent duplication-mediated genome rearrangements. Nature 460: 984–989.

Rattray, A. J., B. K. Shafer, B. Neelam, and J. N. Strathern, 2005 A mechanism of palindromic gene amplification in *Saccharomyces cerevisiae*. Genes Dev. 19: 1390–1399.

Rose, M. D., F. Winston, and P. Hieter, 1990 *Methods in Yeast Genetics*. Cold Spring Harbor Laboratory Press, Cold Spring Harbor, NY.

Rothstein, R., C. Helms, and N. Rosenberg, 1987 Concerted deletions and inversions are caused by mitotic recombination between delta sequences in *Saccharomyces cerevisiae*. Mol. Cell. Biol. 7: 1198–1207.

Sanghani, P. C., W. F. Bosron, and T. D. Hurley, 2002a Human glutathione-dependent formaldehyde dehydrogenase: structural changes associated with ternary complex formation. Biochemistry 41: 15189–15194.

Sanghani, P. C., H. Robinson, W. F. Bosron, and T. D. Hurley, 2002b Human glutathione-dependent formaldehyde dehydrogenase: structures of apo, binary, and inhibitory ternary complexes. Biochemistry 41: 10778–10786.

Schacherer, J., J. de Montigny, A. Welcker, J. L. Souciet, and S. Potier, 2005 Duplication processes in *Saccharomyces cerevisiae* haploid strains. Nucleic Acids Res. 33: 6319–6326.

Schacherer, J., Y. Tourrette, S. Potier, J. L. Souciet, and J. de Montigny, 2007 Spontaneous duplications in diploid *Saccharomyces cerevisiae* cells. DNA Repair 6: 1441–1452.

Scheifele, L. Z., G. J. Cost, M. L. Zupancic, E. M. Caputo, and J. D. Boeke, 2009 Retrotransposon overdose and genome integrity. Proc. Natl. Acad. Sci. USA 106: 13927–13932.

Schiestl, R. H., 1989 Nonmutagenic carcinogens induce intrachromosomal recombination in yeast. Nature 337: 285–288.

Sherman, F., J. W. Stewart, M. Jackson, R. A. Gilmore, and J. H. Parker, 1974 Mutants of yeast defective in iso-1-cytochrome c. Genetics 77: 255–284.

St. Charles, J., E. Hazkani-Covo, Y. Yin, S. L. Andersen, F. S. Dietrich *et al.*, 2012 High-resolution genome-wide analysis of irradiated (UV and gamma rays) diploid yeast cells reveals a high frequency of genomic loss of heterozygosity (LOH) events. Genetics 190: 1267–1284.

Stratton, M. R., P. J. Campbell, and P. A. Futreal, 2009 The cancer genome. Nature 458: 719–724.

Sullivan, P. F., M. J. Daly, and M. O'Donovan, 2012 Genetic architectures of psychiatric disorders: the emerging picture and its implications. Nat. Rev. Genet. 13: 537–551.

Surtees, J. A., J. L. Argueso, and E. Alani, 2004 Mismatch repair proteins: key regulators of genetic recombination. Cytogenet. Genome Res. 107: 146–159.

Szostak, J. W., and R. Wu, 1980 Unequal crossing over in the ribosomal DNA of *Saccharomyces cerevisiae*. Nature 284: 426–430.

Tan, F. J., M. L. Hoang, and D. Koshland, 2012 DNA resection at chromosome breaks promotes genome stability by constraining non-allelic homologous recombination. PLoS Genet. 8: e1002633.

Tang, W., M. Dominska, P. W. Greenwell, Z. Harvanek, K. S. Lobachev *et al.*, 2011 Friedreich's ataxia (GAA)n*(TTC)n repeats strongly stimulate mitotic crossovers in *Saccharomyces cerevisae*. PLoS Genet. 7: e1001270.

Tourrette, Y., J. Schacherer, E. Fritsch, S. Potier, J. L. Souciet *et al.*, 2007 Spontaneous deletions and reciprocal translocations in *Saccharomyces cerevisiae*: influence of ploidy. Mol. Microbiol. 64: 382–395.

Umezu, K., M. Hiraoka, M. Mori, and H. Maki, 2002 Structural analysis of aberrant chromosomes that occur spontaneously in diploid *Saccharomyces cerevisiae*: retrotransposon Ty1 plays a crucial role in chromosomal rearrangements. Genetics 160: 97–110.

Veltman, J. A., and H. G. Brunner, 2012 De novo mutations in human genetic disease. Nat. Rev. Genet. 13: 565–575.

Vernon, M., K. Lobachev, and T. D. Petes, 2008 High rates of "unselected" aneuploidy and chromosome rearrangements in *tel1 mec1* haploid yeast strains. Genetics 179: 237–247.

Watanabe, T., and T. Horiuchi, 2005 A novel gene amplification system in yeast based on double rolling-circle replication. EMBO J. 24: 190–198.

Wei, W., J. H. McCusker, R. W. Hyman, T. Jones, Y. Ning *et al.*, 2007 Genome sequencing and comparative analysis of *Saccharomyces cerevisiae* strain YJM789. Proc. Natl. Acad. Sci. USA 104: 12825–12830.

Welch, J. W., D. H. Maloney, and S. Fogel, 1990 Unequal crossing-over and gene conversion at the amplified *CUP1* locus of yeast. Mol. Gen. Genet. 222: 304–310.

Wijchers, P. J., and W. de Laat, 2011 Genome organization influences partner selection for chromosomal rearrangements. Trends Genet. 27: 63–71.

Communicating editor: C.-ting Wu

GENETICS

Supporting Information
http://www.genetics.org/lookup/suppl/doi:10.1534/genetics.112.146522/-/DC1

Gene Copy-Number Variation in Haploid and Diploid Strains of the Yeast *Saccharomyces cerevisiae*

Hengshan Zhang, Ane F. B. Zeidler, Wei Song, Christopher M. Puccia, Ewa Malc, Patricia W. Greenwell, Piotr A. Mieczkowski, Thomas D. Petes, and Juan Lucas Argueso

DOI: 10.1534/genetics.112.146522

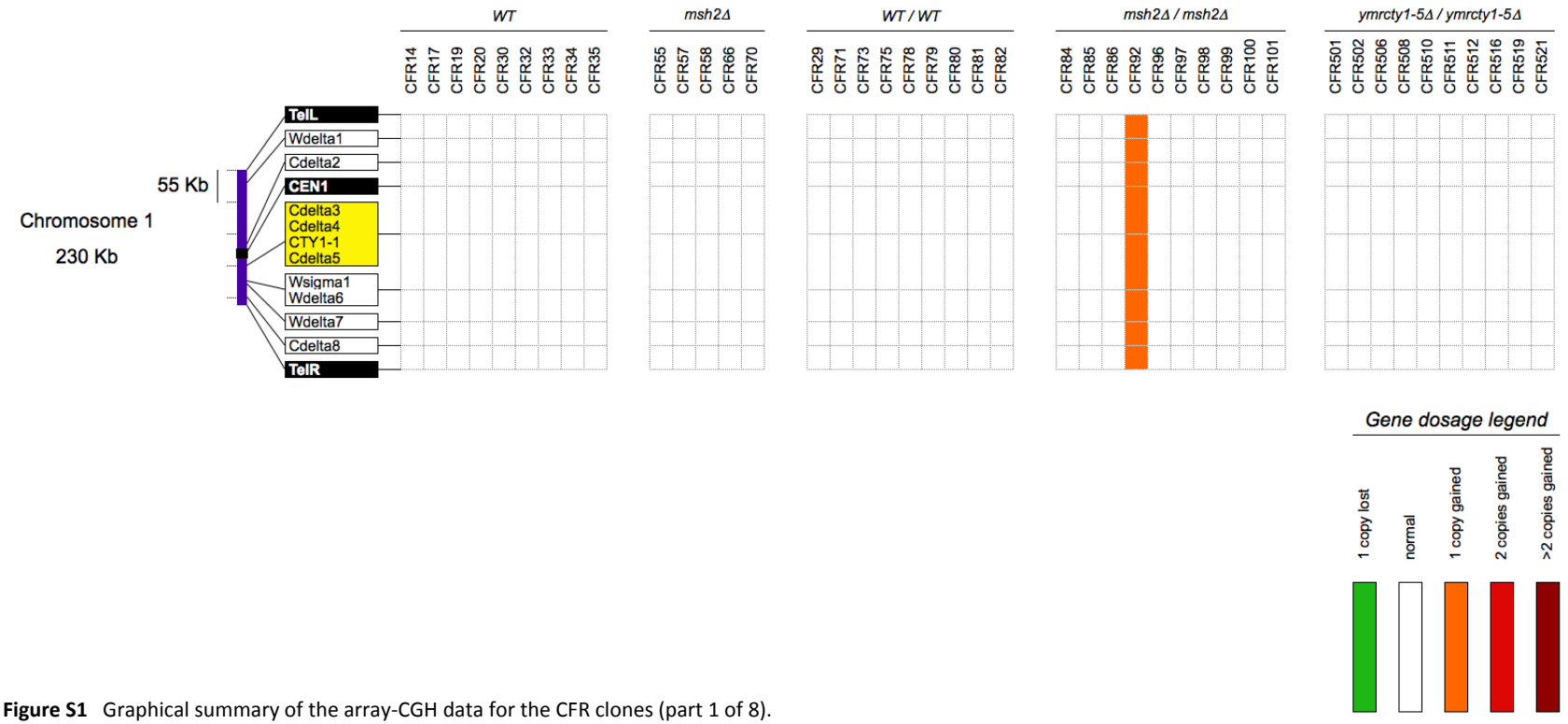

Figure S1 Graphical summary of the array-CGH data for the CFR clones (part 1 of 8).

The panels show a graphical representation of the deletion and amplification events detected by array-CGH for each chromosome. Only the chromosomes for which CNVs were detected are shown. The columns correspond to individual FA/Cu resistant isolates, the corresponding genotype of haploids or diploids is also indicated.
Each row in the tables corresponds to a Ty-containing site or an LTR-containing site that is annotated in the S288c reference genome sequence available at the Saccharomyces Genome Database (SGD). Tys and LTRs are frequently clustered and in this analysis they appear as a groups since our microarrays do not have the resolution to discriminate the hybridization signal from each individual part of the cluster. A cluster means that there are no probes of non-repetitive DNA between each feature. Sites containing full-length Ty1 and/or Ty2 insertions are highlighted in yellow. Sites containing solo LTRs and/or full length Ty3, Ty4 and Ty5 insertions are not highlighted. The site containing the *SFA1-CUP1* CNV reporter genes on Chr5 is highlighted in blue. The columns are colored to indicate that an alteration of gene dosage was detected by the array-CGH in the corresponding interval. The gene dosage changes are color-coded according to the legend above, and specifically: Bright green = -1 copy relative to parent haploid or diploid; White (or no color) = no dose change; Orange = +1 copy relative to parent (2 copies in haploids, and 3 copies in diploids); Red = +2 copies relative to parent (3 copies in haploids, and 4 copies in diploids); Brown = +3 or more copies relative to parent (4 or more copies in haploids, and 5 or more copies in diploids). The extent of the colored bars corresponds to the chromosomal region where the dose change occurred, and it indicates the specific boundaries for dosage change (breakpoints). Aneuploidy events are shown as the entire chromosome colored from telomere to telomere.

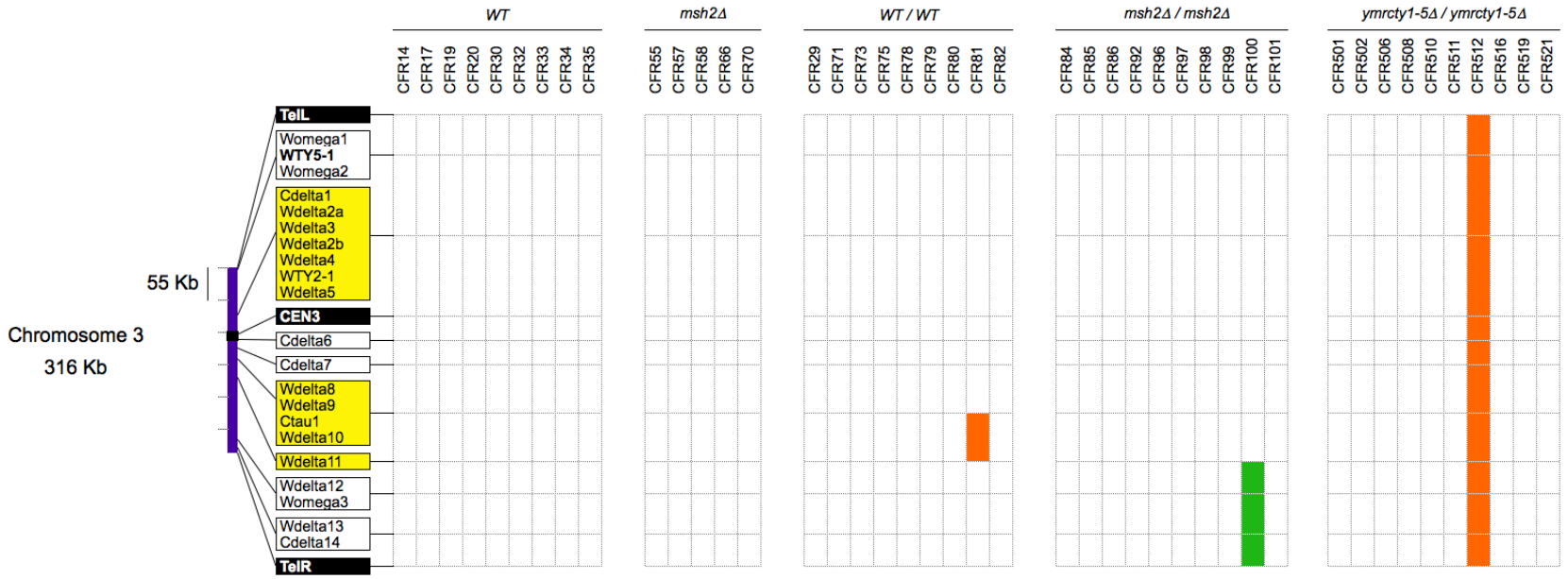

Figure S1 Graphical summary of the array-CGH data for the CFR clones (continued; part 2 of 8).

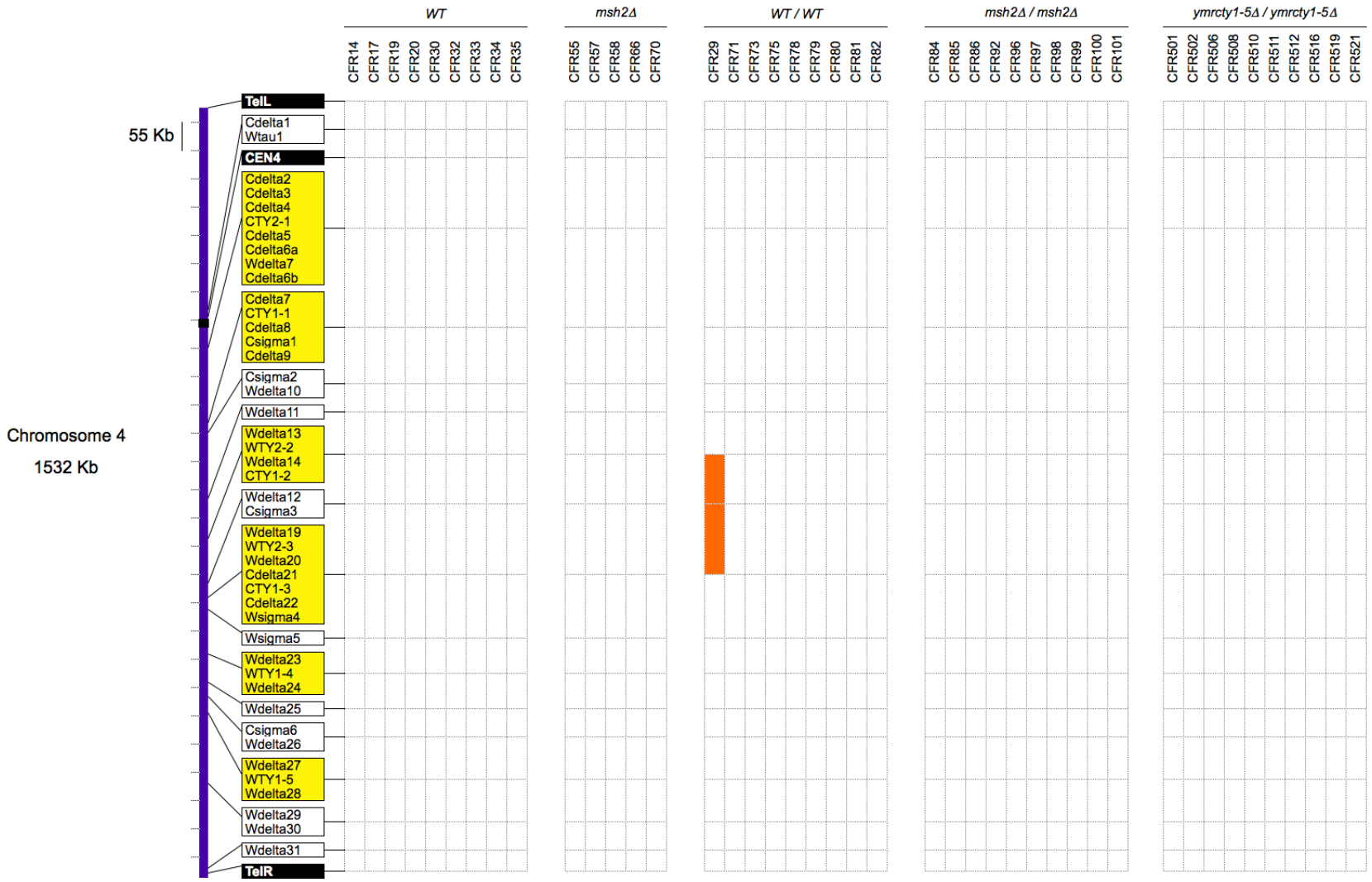

Figure S1 Graphical summary of the array-CGH data for the CFR clones (continued; part 3 of 8).

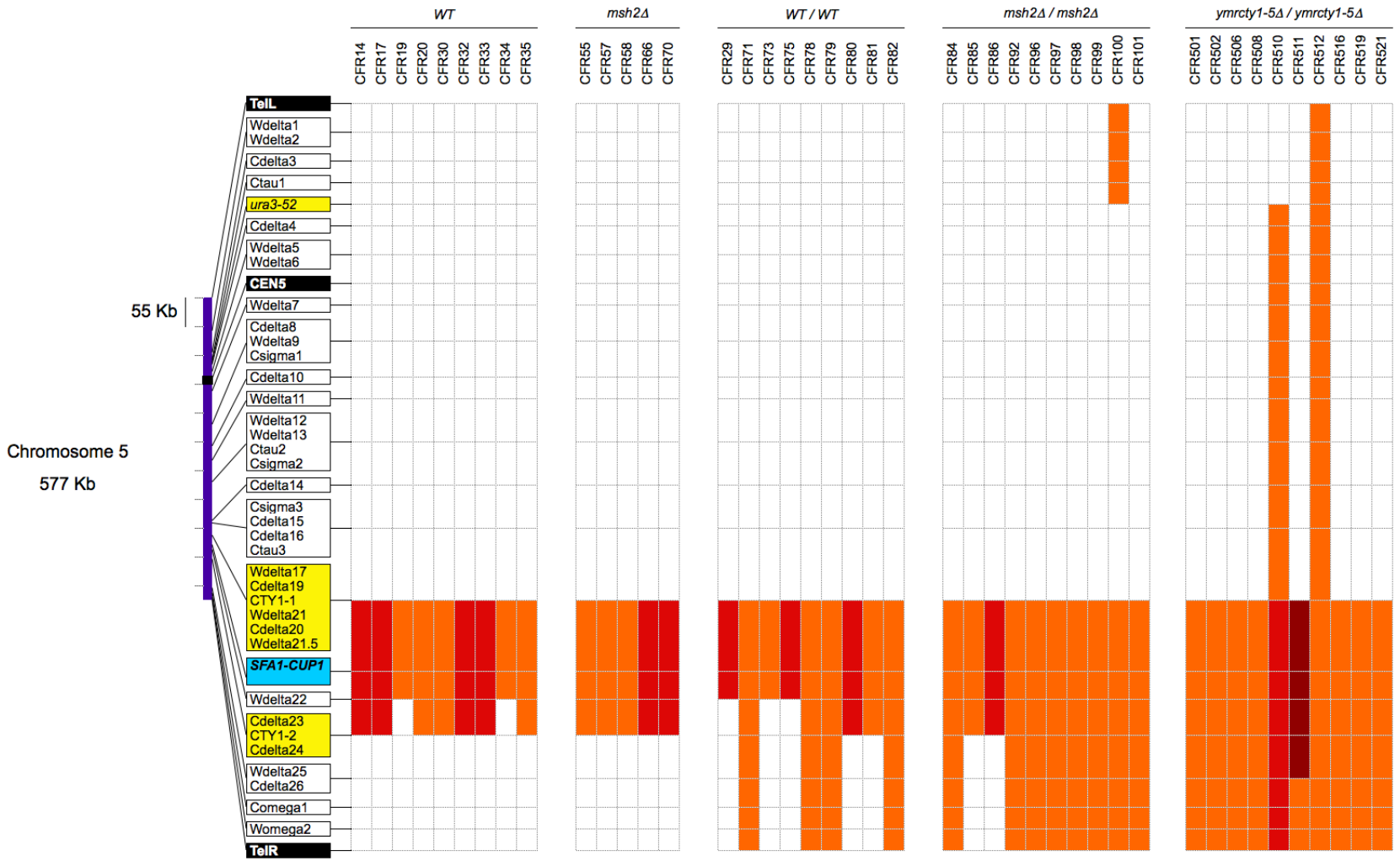

Figure S1 Graphical summary of the array-CGH data for the CFR clones (continued; part 4 of 8).

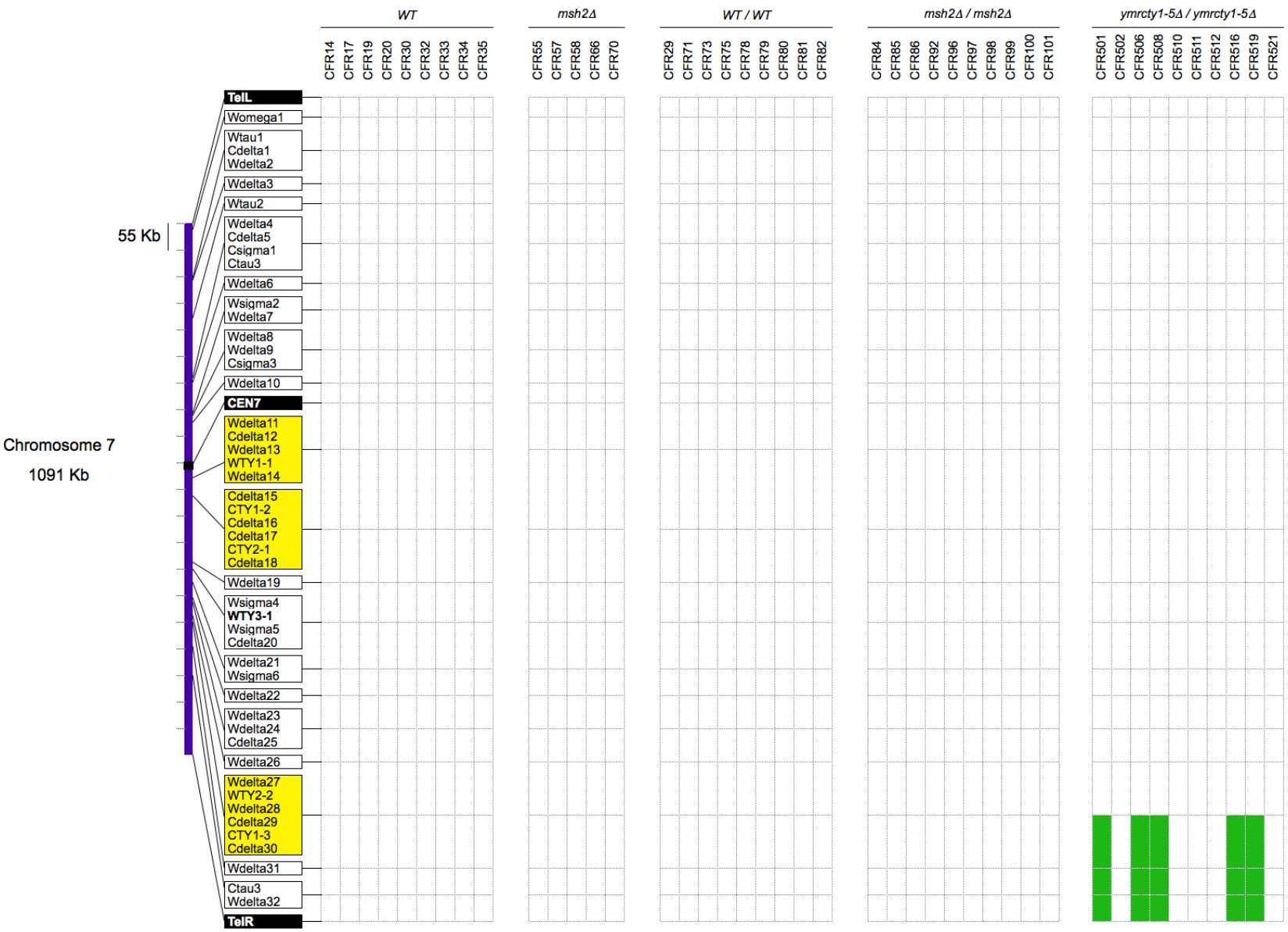

Figure S1 Graphical summary of the array-CGH data for the CFR clones (continued; part 5 of 8).

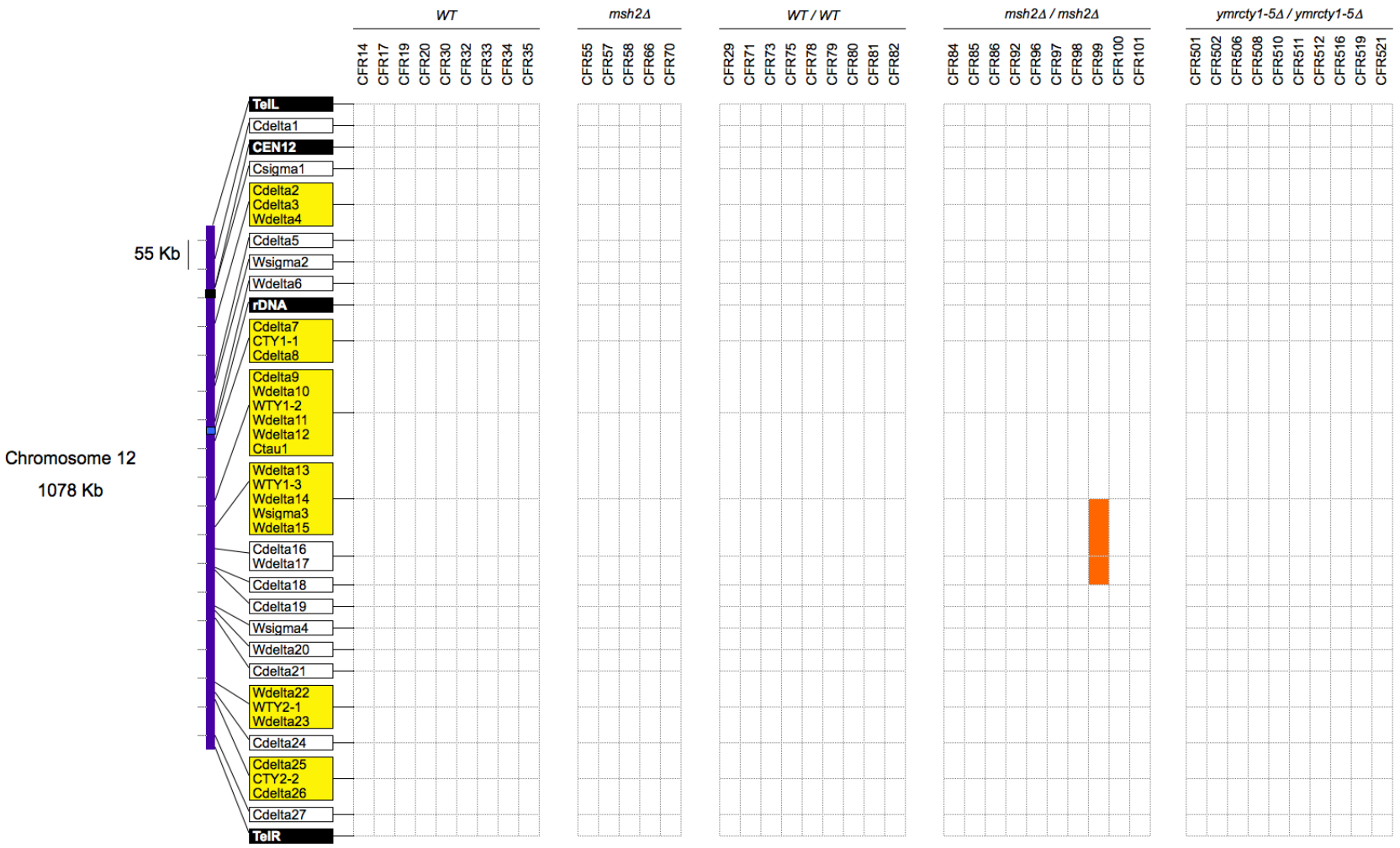

Figure S1 Graphical summary of the array-CGH data for the CFR clones (continued; part 6 of 8).

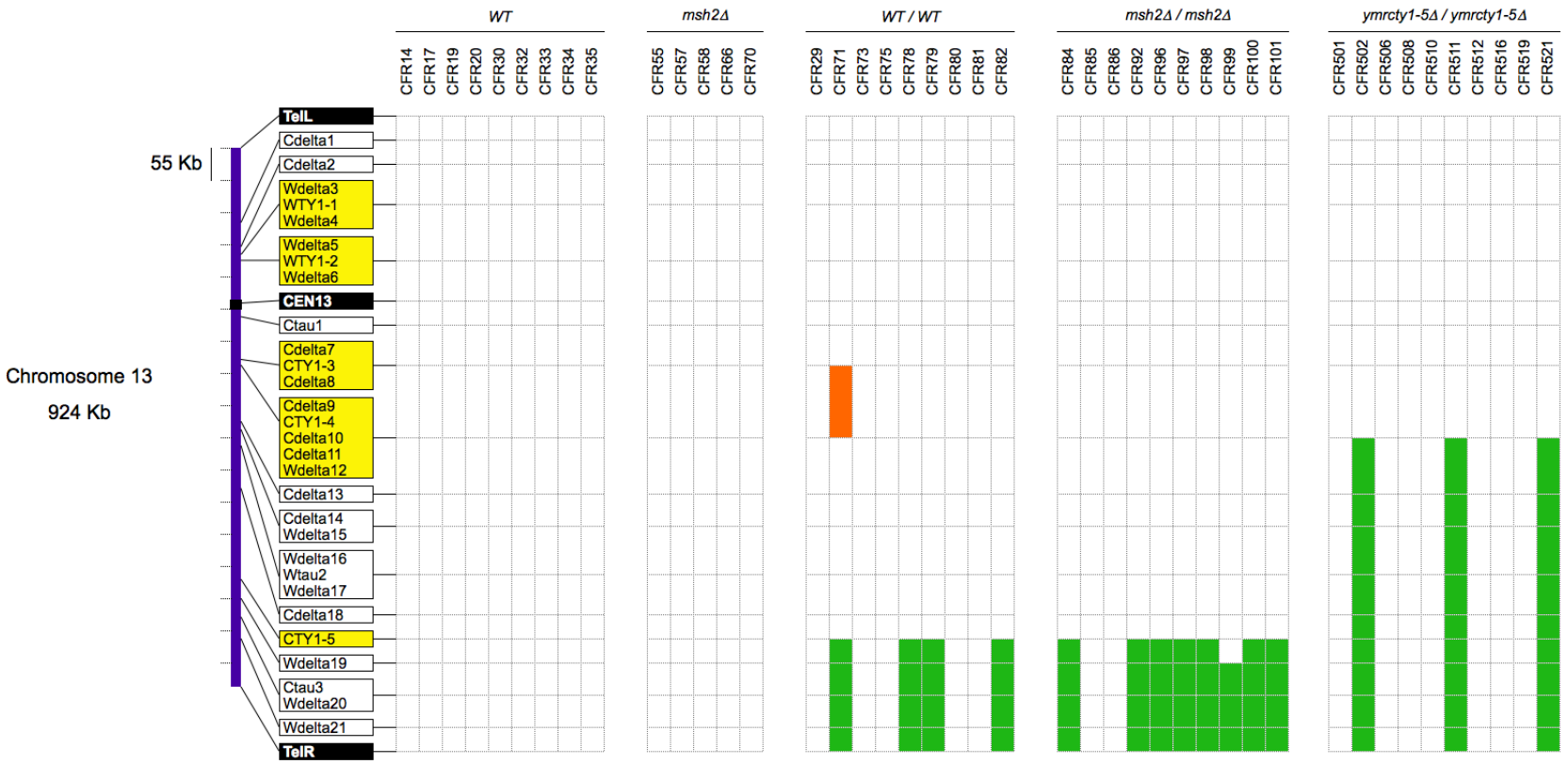

Figure S1 Graphical summary of the array-CGH data for the CFR clones (continued; part 7 of 8).

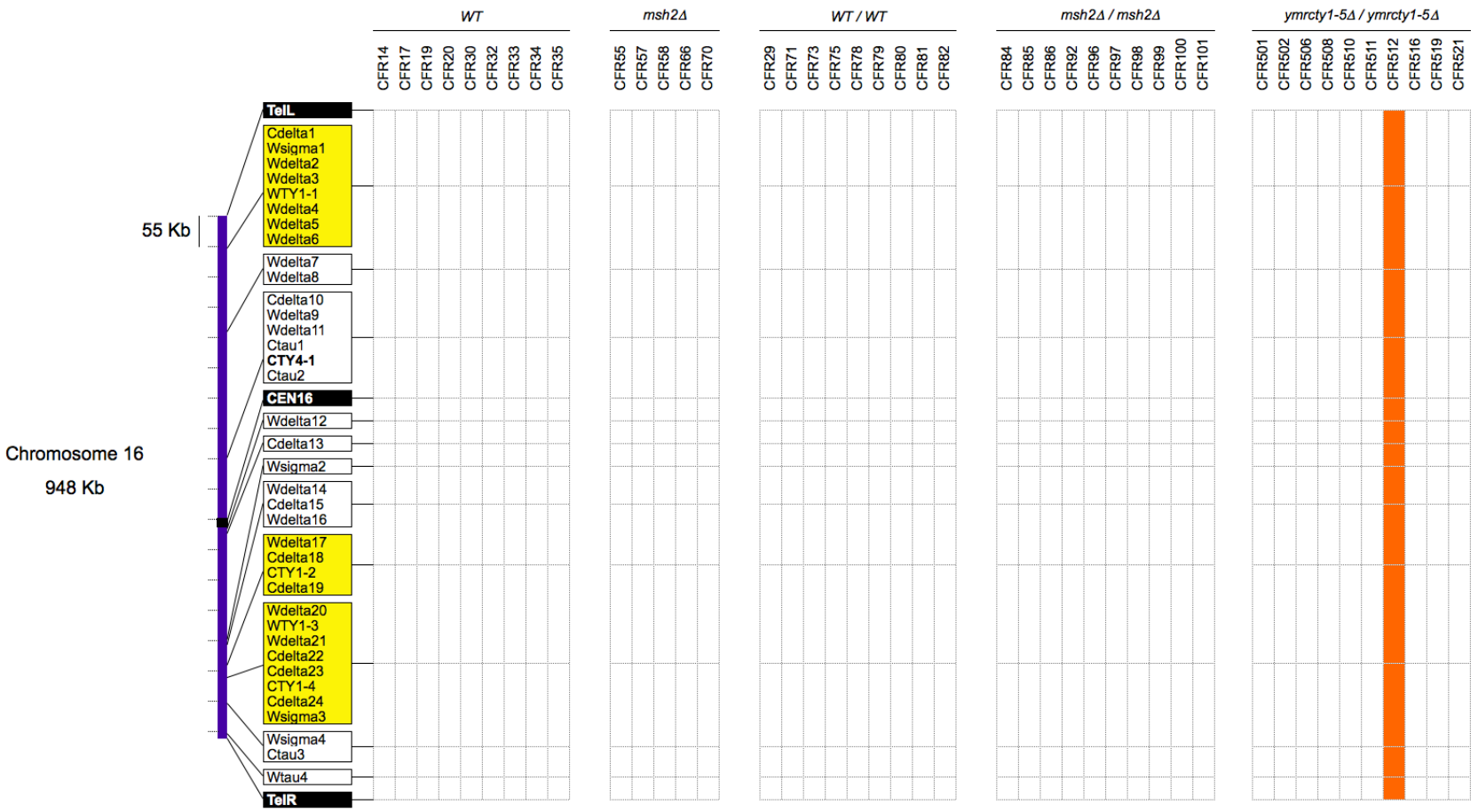

Figure S1 Graphical summary of the array-CGH data for the CFR clones (continued; part 8 of 8).

A

Haploid strains	Copies of *SFA1-CUP1*		
	Chr4	Chr5	Total
JAY357	0	0	**0**
JAY247	1	0	**1**
JAY372	0	1	**1**
JAY381	1	1	**2**

B

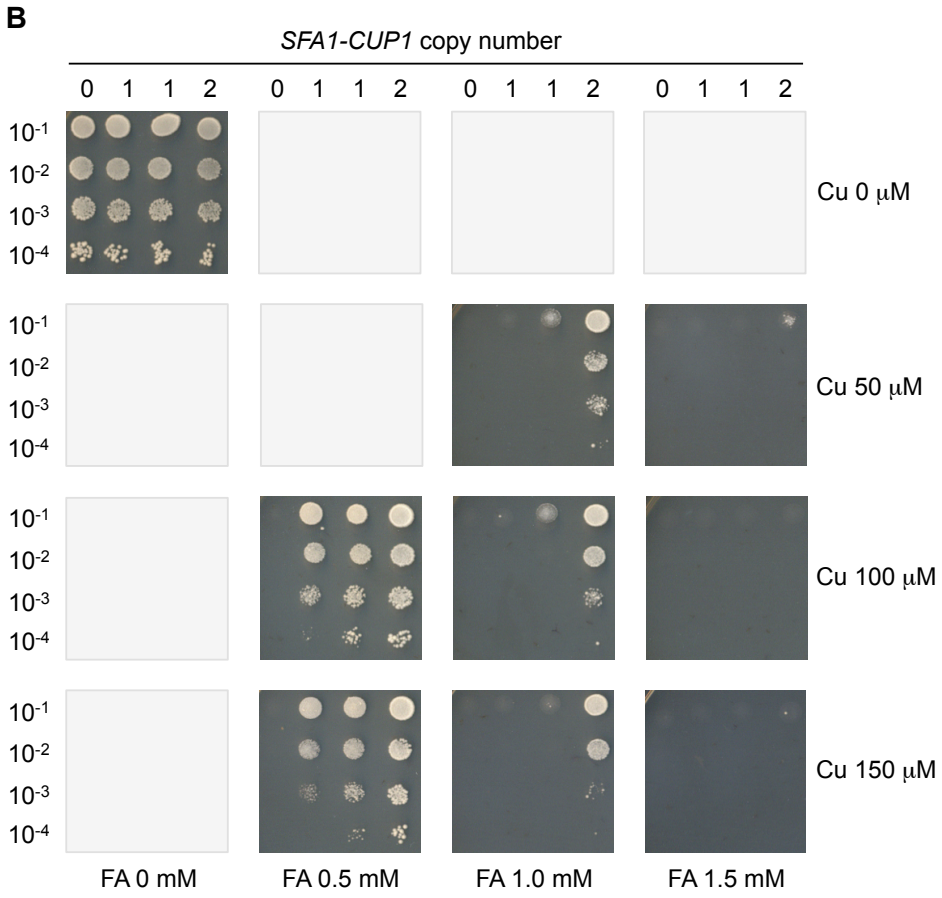

Figure S2 FA and Cu concentration optimization trials: Haploids.

(A) Haploid strains used in the optimizations trials. The table shows the total copy number of the *SFA1-CUP1* reporter, and the site of reporter insertion in the genome. The Chr4 site is the *SFA1* locus and the Chr5 site is the *DDI1* locus.
(B) Representative reporter dosage-dependent resistance to different combinations of FA and Cu concentrations. Serial dilutions of strains JAY357, JAY247, JAY372, and JAY381 shown in (A) were spotted in this order, from left to right. Cells were grown for 3 days at 30^{o}. Note that at equal dose, the Chr4 reporter insertion confers slightly lower resistance to FA/Cu than the Chr5 insertion, presumably due to a small difference in basal gene expression. The gray squares represent FA/Cu combinations not tested in this specific trail.

A

Diploid strains	Copies of *SFA1-CUP1*		
	Chr4	Chr5	Total
JAY275	0	0	**0**
JAY386	0	1	**1**
JAY350	0	2	**2**
JAY384	1	2	**3**
JAY385	2	2	**4**

B

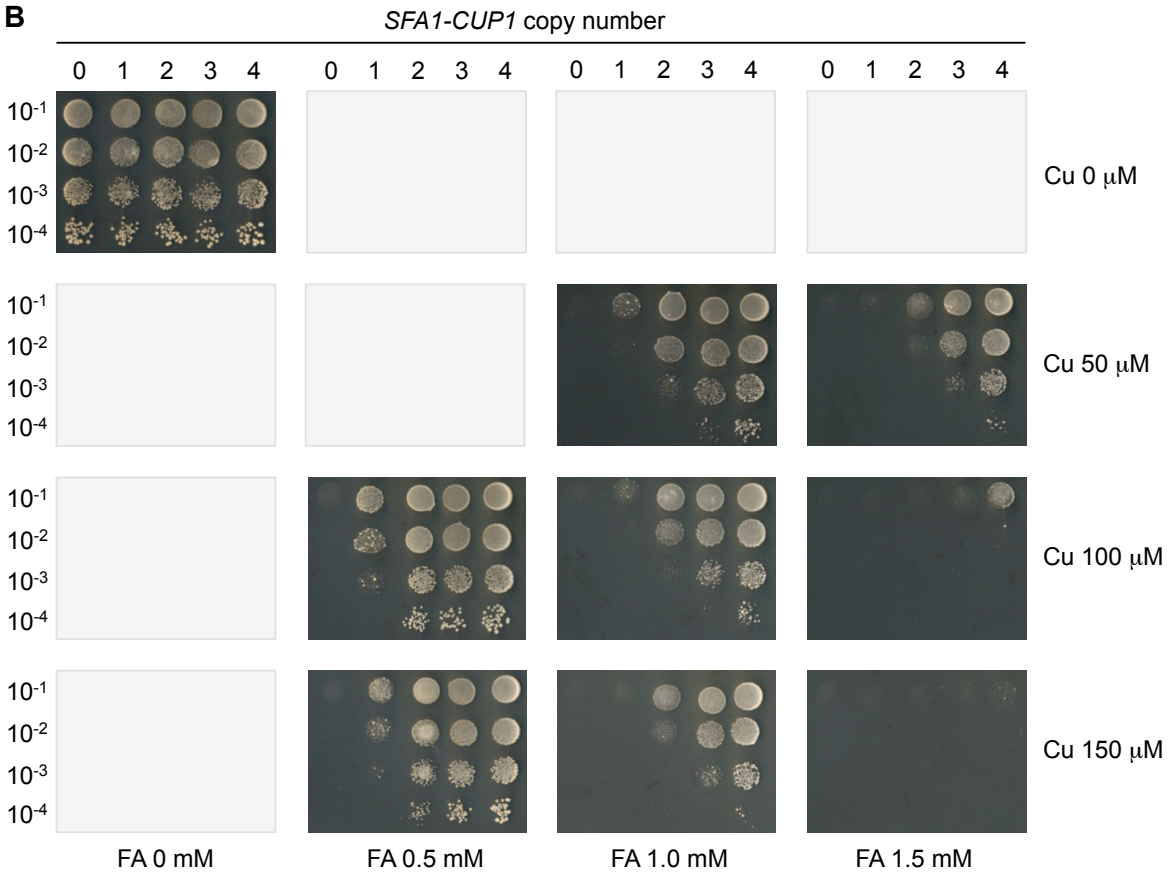

Figure S3 FA and Cu concentration optimization trials: Diploids.

(A) Diploid strains used in the optimizations trials. The table shows the total copy number of the *SFA1-CUP1* reporter, and the site of reporter insertion in the genome. The Chr4 site is the *SFA1* locus and the Chr5 site is the *DDI1* locus.
(B) Representative reporter dosage-dependent resistance to different combinations of FA and Cu concentrations. Serial dilutions of strains JAY275, JAY386, JAY350, JAY384, and JAY385 shown in (A) were spotted in this order, from left to right. Cells were grown for 3 days at 30°. The gray squares represent FA/Cu combinations not tested in this specific trail.

A

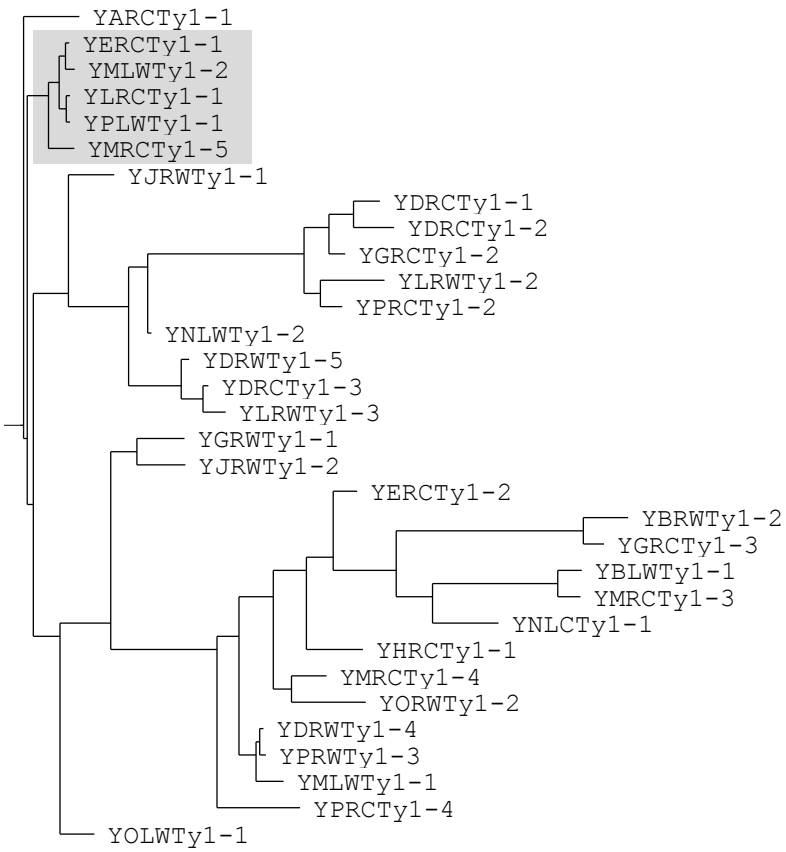

B

Ty1 element	Alignment size	Number of mismatches	Longest perfect match
YMLWTy1-2	5890	3	3708
YLRCTy1-1	5922	12	2138
YPLWTy1-1	5924	11	2138
YMRCTy1-5	5903	25	2981

Figure S4 Nucleotide sequence similarity between Ty1 elements.

(A) Sequence similarity tree between all full length Ty1 retrotransposon elements annotated in the S288c genome, also including the un-annotated *YMRCTy1-5* element on the right arm of Chr13. The cluster of Ty1 elements most similar to *YERCTy1-1* is shaded in gray. (B) Sequence identity parameters between *YERCTy1-1* and the four other Ty1 elements most similar to it in the genome. Values are given in base pairs (bp).

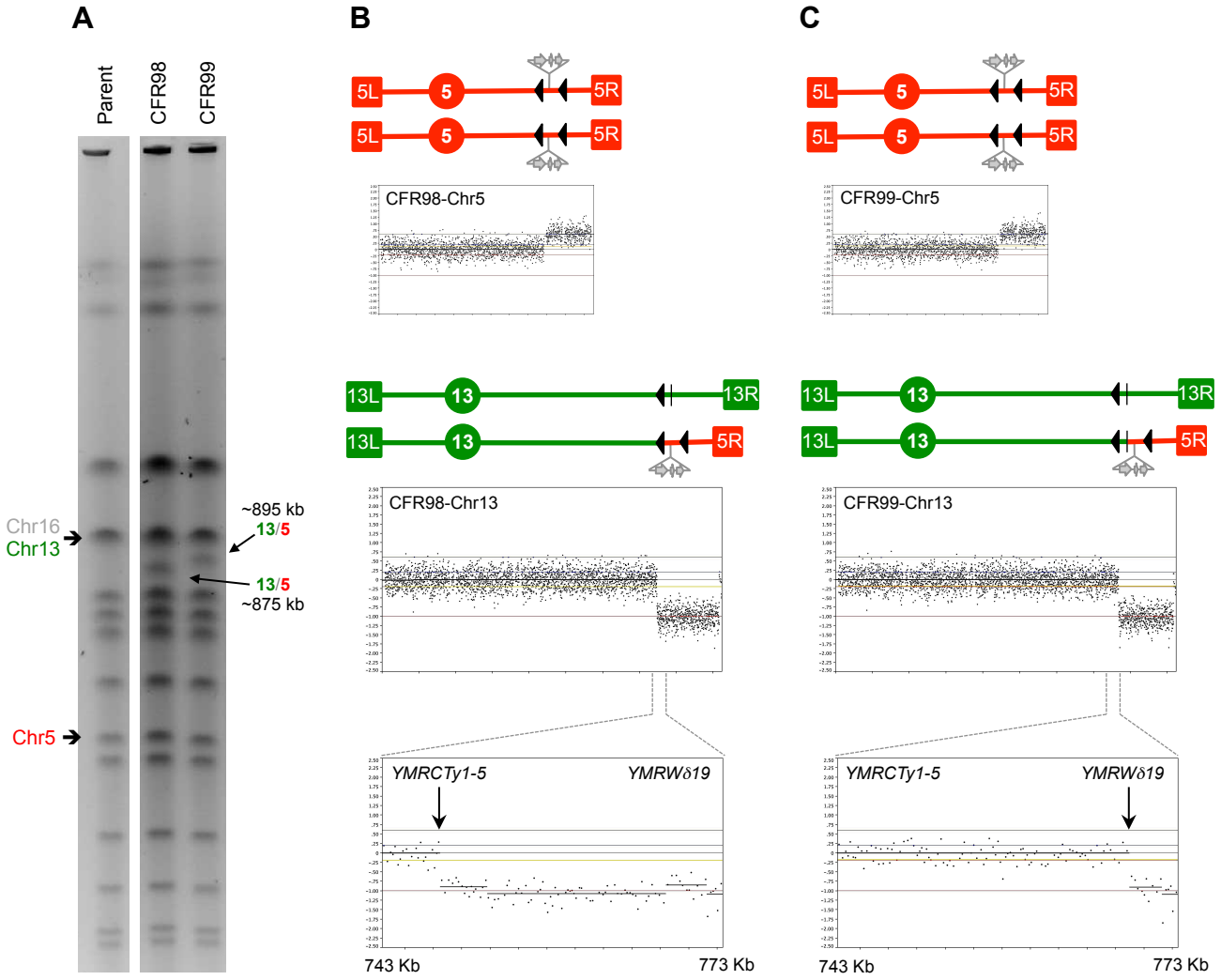

Figure S5 Chr13/Chr5 translocations in two CFR clones isolated from *msh2Δ/msh2Δ* diploids.

(A) PFGE showing the karyotypes of CFR98 and CFR99, with their respective Chr13/Chr5 translocations indicated.
(B) and (C) array-CGH and schematic representation of the Chr13/Chr5 translocations in CFR98 and CFR99, respectively. The black arrowheads represent full length Ty1 elements, the vertical thin black line represents the *YMRWδ19* LTR on Chr13. The Chr5 breakpoints are near the *YERCTy1-1* / *YERWδ20B* region in both clones. The array-CGH plots at the bottom of the panels show the expanded view of the 40 kb Chr13 region where deletion breakpoints (black arrows) were detected in each clone. The deletion in CFR98 starts at *YMRCTy1-5*, whereas the deletion in CFR99 starts ~20 kb to the right at *YMRWd19*.

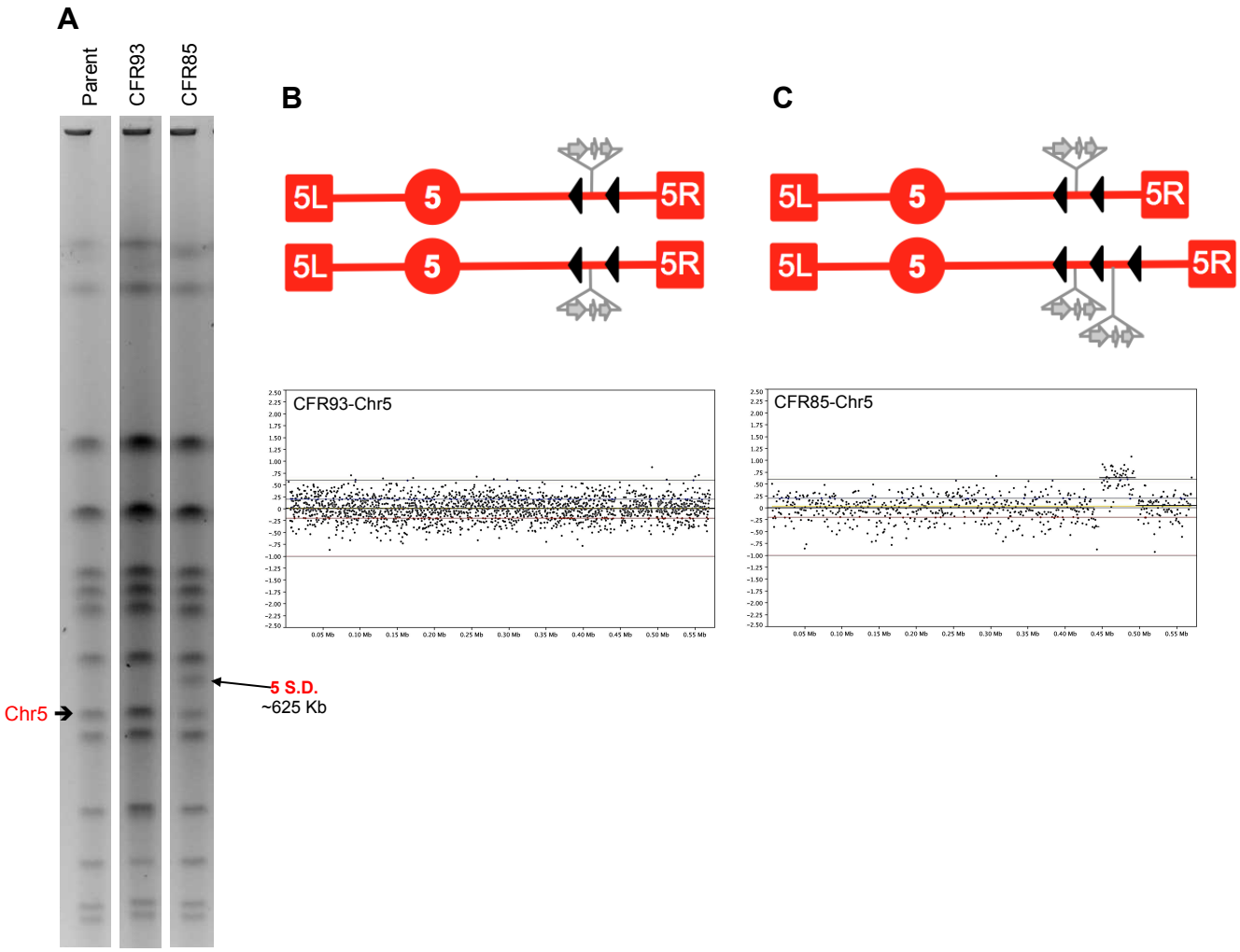

Figure S6 CNV-less and segmental duplication CFR clones isolated from *msh2Δ/msh2Δ* diploids.

(A) PFGE showing the karyotypes of CFR93 (no visible karyotype changes) and CFR85, which shows a parental Chr5 band at approximately half the normal abundance (single copy), and a larger Chr5 band containing a segmental duplication.
(B) array-CGH and schematic representation of Chr5 CFR93. CFR93 does not show any gene dose changes in this chromosome or anywhere else in the genome. Instead, CFR93 was identified in the assay due to the presence of a dominant point mutation in the *SFA1* gene.
(C) array-CGH and schematic representation of Chr5 CFR85. CFR85 contains a parental copy of Chr5 and the second homolog contains a segmental duplication between *YERCTy1-1* and *YERCTy1-2*.

File S1

Supporting Materials and Methods

Detailed description of yeast strains and plasmids:

The *CUP1* locus contains several copies of a tandem ~2 kb repeat structure that includes one copy of the *CUP1* gene and one copy of gene *YHR154C*. *YHRC154C* is identical to the 3' end of the *RSC30* gene, the gene located immediately distal to the *CUP1* locus (right side). Therefore, the rightmost repeat unit in the *CUP1* locus overlaps the *RSC30* gene. To obtain a complete deletion of the *CUP1* repeats without disturbing *RSC30* (which plays roles in chromatin remodeling and DNA double strand break repair (SHIM *et al.* 2005)), we modified the *CUP1* locus in two steps. We first deleted all *CUP1* repeats (including the 3' end of *RSC30*) through integration of a PCR fragment containing the *Kl*URA3-*Kan*MX4 CORE cassette (primers JAO99/JAO100; template pCORE (STORICI *et al.* 2001)), followed by transformation with a PCR product that removed the CORE cassette and restored the 3' end of *RSC30* (JAO101/JAO102; WT genomic DNA template). The resulting allele (*cup1Δ RSC30*) had no copies of *CUP1* and one intact copy of *RSC30*, and corresponded to a deletion that included SGD Chr8 coordinates 212,262 to 215,159.

To delete the *SFA1* gene, we built a plasmid (pJA35) containing the *hisG-URA3-hisG* cassette (ALANI *et al.* 1987) flanked by homology regions from both sides of *SFA1*. The homology regions were amplified by PCR from genomic DNA corresponding to SGD Chr4 coordinates 158,742 to 159,349 (JAO326/JAO327; introducing 5' *Eco*RI and 3' *Bam*HI sites) and 160,824 to 160,994 (JAO328/JAO329; introducing 5' *Bam*HI and 3' *Sal*I sites). These two products were digested with *Bam*HI and ligated. A 825 bp ligation product was purified, digested with *Eco*RI and *Sal*I, and ligated to an *Eco*RI/*Sal*I digested pUC19 cloning vector. The resulting plasmid (pJA34) was digested with *Bam*HI, the ends were treated with calf intestinal alkaline phosphatase (CIP), and ligated to a *Bam*HI/*Bgl*II fragment from pNKY51 containing the *hisG-URA3-hisG* cassette (ALANI *et al.* 1987). The resulting pJA35 plasmid was linearized with *Eco*RI and *Sal*I prior to integration into the yeast genome at the *SFA1* locus (*sfa1Δ::hisG-URA3-hisG*), and subsequently a spontaneous *URA3* pop-out event was selected on 5-FOA. The resulting *sfa1Δ::hisG* allele corresponded to a deletion of SGD Chr4 coordinates 159,350 to160,823. The *msh2Δ::hisG* deletion was generated using a similar strategy, through integration of a fragment from linearized plasmid pEAI98, a generous gift from Eric Alani.

The *YMRCTy1-5* element was identified previously as a Ty1 element present in CG379, but absent in the S288c reference genome (ARGUESO *et al.* 2008). We amplified this element by PCR from genomic DNA with primers JAO291/JAO294 and sequenced the product. *YMRCTy1-5* is inserted at the equivalent SGD Chr13 coordinate 748,219. We deleted this element by integration of a PCR product containing the *Kl*URA3-*Kan*MX4 CORE cassette (*ymrcty1-5Δ::CORE*; primers JAO510/JAO511; template pCORE (STORICI *et al.* 2001)), but in this case we did not carry out the secondary transformation to remove CORE.

The *SFA1-CUP1-Hph*MX4 CNV reporter cassette was constructed as follows. Plasmid pAG32 containing the *Hph*MX4 Hygromycin B resistance marker (GOLDSTEIN and MCCUSKER 1999) was linearized with *Bgl*II and ligated to a *Bgl*II digested PCR product containing the *CUP1* gene (JAO104/JAO105; genomic DNA template; 5' and 3' *Bgl*II sites). This plasmid (pJA22) has a 776 bp insertion of *CUP1* including its upstream and downstream regulatory regions (SGD Chr8 coordinates 212,363 to 213,139) in the same transcriptional orientation as the *Hph* marker. pJA22 was used as template to amplify a PCR product (primers JAO113/JAO114) that was integrated into the yeast genome downstream of the *SFA1* gene between SGD Chr4 coordinates 160,823 and 160,842 (*SFA1::CUP1-Hph*MX4). Finally, genomic DNA containing this insertion was used as template to amplify a PCR product (primers JAO143/JAO269) that was integrated on Chr5, between the *DDI1* and *UBP5* genes, at SGD coordinate 457,705 (*DDI1::SFA1-CUP1-Hph*MX4). The cassette includes

a segment of *SFA1* corresponding to SGD Chr4 coordinates 159,349 to 160,823, and includes 255 bp of the *SFA1* native promoter. We also generated a version of the CNV reporter marked with G418 resistance by integrating a *Kan*MX4 PCR product (JAO457/JAO458; pFA6-KanMX4 template (WACH *et al.* 1994)) at the site where *Hph*MX4 was originally found, resulting in the *DDI1::SFA1-CUP1-Kan*MX4 marker swap reporter.

In addition to the genetic modifications above constructed for the CNV assay, we also produced constructs that were used to examine allelic mitotic recombination on the right arm of Chr13. We integrated the *KlURA3-Kan*MX4 CORE cassette on the CG379 strain background near the right end of Chr13, at a position distal to the *ADH6* gene, between SGD coordinates 910,882 and 910,902 (*ADH6::CORE*; JAO502/JAO503; template pCORE (STORICI *et al.* 2001)). The resulting strain (JAY405) was mated to the diverged strain YJM799 (isogenic to YJM789 (WEI *et al.* 2007)) to generate the hybrid diploid JAY408.

We also created a similar hybrid diploid that had an integration of a modified version of the original CORE cassette at the same Chr13 position. We created plasmid pJA40 that contains a copy of the *S. cerevisiae URA3* gene (*ScURA3*) in addition to the *KlURA3* marker already present in the original pCORE. The presence of two different, but functionally redundant copies of *URA3* improved the sensitivity of the cells to 5-FOA, and eliminated the occurrence of resistant clones that originate through base pair mutation in *KlURA3*. Strains carrying a CORE2 insertion (*KlURA3-ScURA3-KanMX4*) can only become resistant to 5-FOA following simultaneous inactivation of both copies of *URA3*, possible through a genome rearrangement or LOH event, or extremely rarely through point mutations in both *URA3* genes. pJA40 was constructed by linearizing pCORE with *Bgl*II and *Xma*I. The wild type *ScURA3* gene was amplified from genomic DNA of Ura$^+$ strain JAY291 (ARGUESO *et al.* 2009) using primers JAO336 and JAO650 which had a *Bgl*II site added to the 5' end. This PCR product was then digested with *Bgl*II and *Xma*I and ligated to the pCORE backbone. The resulting pJA40 includes a 1.1 kb fragment (SGD Chr5 coordinates 115,949 to 117,047) that includes the Sc*URA3* gene and its native regulatory regions; and because *ScURA3* was inserted between *KlURA3* and *Kan*, primers originally designed to amplify the CORE cassette also work for CORE2 PCR.

Prior to integration of CORE2 into the genome, we created a derivative of CG379 in which the existing *ura3-52* mutation was replaced with a full deletion of the locus. We first repaired *ura3-52* by transforming a PCR product containing the wild type *URA3* gene from JAY291 (primers JAO487/JAO490) and selecting for the Ura$^+$ phenotype. This Ura$^+$ intermediate strain was transformed with an overlapping PCR product (JAO863/JAO866) that joined two fragments corresponding to sequences upstream (JAO863/JAO864) and downstream (JAO865/JAO866) of *URA3*, followed by selection for 5-FOA resistance. The resulting strain contained a deletion of the *URA3* locus (*ura3Δ0* allele), corresponding to the deletion of SGD Chr5 coordinates 116,069 and 117,036. This strain was used to integrate the CORE2 cassette near the right end of Chr13 (*ADH6::CORE2*; JAO502/JAO503; template pJA40), resulting in strain JAY794 that was mated to YJM799 to generated the hybrid diploid JAY800.

Molecular karyotyping analysis: PFGE and array-CGH:

Yeast cultures were grown in 7 ml liquid YPD at 30^o for 48 hr. The cells were then immobilized in LMP-agarose plugs to prepare full-length chromosomal DNA for PFGE. Ten plugs were prepared for each clone. Genomic DNA for array-CGH was prepared by extraction from the same agarose plug batches prepared for PFGE. This was ensure that the PFGE and array-CGH analyses were done using the same DNA preparation, minimizing the effects of differential loss of unstable chromosomal rearrangements between independent DNA preparation cultures. To prepare genomic DNA for array-CGH, we briefly dried four PFGE agarose plugs (~70 μl each) with paper wipes to remove excess 1x TE storage buffer and transferred them to a 15 ml polypropylene conical tube. The DNA was purified using a modified Fermentas GeneJET gel extraction kit protocol. 280 μl of binding buffer was added to melt the agarose plugs.

Tubes were vortexed to homogenize the suspension and then transferred to a Diagenode Bioruptor UCD-200 multisample sonicator to shear the DNA. The tubes were incubated for 30 minutes at 4°, at high power setting, and cycles of 30 sec ON and 30 sec OFF. After sonication, the normal Fermentas-recommended gel extraction protocol was followed, concluding with collection of the sheared DNA in 20 μl of elution buffer. The size of the sheared fragments (typically 1-2 kb) was examined in a 1% agarose gel, and the DNA concentration (typically 150-250 ng/μl) was measured in an Invitrogen Qubit fluorometer. DNA from the parental strain was prepared using the same protocol. One μg of sheared CFR clone DNA was labeled with dUTP-Cy5 (GE-Healthcare) using the Invitrogen BioPrime array-CGH labeling system, and parental DNA was labeled with dUTP-Cy3. The labeled DNAs were co-hybridized to one of two types of Agilent microarrays designs. Agilent catalog design G4810A-14810 slides have four array sectors (4x44k), each with 41,775 60-nucleotide single stranded probes distributed across the genome with a median spacing of 257 bp. We also used lower density custom-designed Agilent slides that had eight array sectors per slide (8x15k), each containing essentially every third probe from the 4x44k catalog design, totaling 14,965 probes and a median spacing of 774 bp. This custom 8x15k design (AMID 028943) has sufficient genomic coverage to locate CNV breakpoints at a resolution comparable to that of the higher density 4x44k catalog design. The hybridized microarray slides were scanned and the hybridization signal was quantified with Genepix 6.0 software. Subsequently, the hybridization data was analyzed with Biodiscovery Nexus Copy Number software to identify the CNVs present in each CFR.

Supporting cited literature:

ALANI, E., L. CAO and N. KLECKNER, 1987 A method for gene disruption that allows repeated use of *URA3* selection in the construction of multiply disrupted yeast strains. Genetics **116:** 541-545.

ARGUESO, J. L., M. F. CARAZZOLLE, P. A. MIECZKOWSKI, F. M. DUARTE, O. V. C. NETTO *et al.*, 2009 Genome structure of a *Saccharomyces cerevisiae* strain widely used in bioethanol production. Genome Research **19:** 2258-2270.

ARGUESO, J. L., J. WESTMORELAND, P. A. MIECZKOWSKI, M. GAWEL, T. D. PETES *et al.*, 2008 Double-strand breaks associated with repetitive DNA can reshape the genome. Proceedings of the National Academy of Sciences of the United States of America **105:** 11845-11850.

GOLDSTEIN, A. L., and J. H. MCCUSKER, 1999 Three new dominant drug resistance cassettes for gene disruption in *Saccharomyces cerevisiae*. Yeast **15:** 1541-1553.

SHIM, E. Y., J. L. MA, J. H. OUM, Y. YANEZ and S. E. LEE, 2005 The yeast chromatin remodeler RSC complex facilitates end joining repair of DNA double-strand breaks. Molecular and Cellular Biology **25:** 3934-3944.

STORICI, F., L. K. LEWIS and M. A. RESNICK, 2001 In vivo site-directed mutagenesis using oligonucleotides. Nature Biotechnology **19:** 773-776.

WACH, A., A. BRACHAT, R. POHLMANN and P. PHILIPPSEN, 1994 New heterologous modules for classical or PCR-based gene disruptions in *Saccharomyces cerevisiae*. Yeast **10:** 1793-1808.

WEI, W., J. H. MCCUSKER, R. W. HYMAN, T. JONES, Y. NING *et al.*, 2007 Genome sequencing and comparative analysis of *Saccharomyces cerevisiae* strain YJM789. Proceedings of the National Academy of Sciences of the United States of America **104:** 12825-12830.

Table S1 Yeast strains used in this study

Strains[a]:	Genotypes[b]:					
FA/Cu resistance gene amplification assay						
Haploids:						
JAY357:	*MATα*	*cup1Δ RSC30*	*sfa1Δ::hisG*			
JAY247:	*MATα*	*cup1Δ RSC30*	*SFA1::CUP1-HphMX4*			
JAY381:	*MATα*	*cup1Δ RSC30*	*SFA1::CUP1-HphMX4*	*DDI1::SFA1-CUP1-HphMX4*		
JAY372:	*MATα*	*cup1Δ RSC30*	*sfa1Δ::hisG*	*DDI1::SFA1-CUP1-HphMX4*		
JAY378:	*MATα*	*cup1Δ RSC30*	*sfa1Δ::hisG*	*DDI1::SFA1-CUP1-KanMX4*		
HSZy1 and HSZy2[c]:	*MATα*	*cup1Δ RSC30*	*sfa1Δ::hisG*	*DDI1::SFA1-CUP1-KanMX4*	*msh2Δ::hisG*	
Diploids:						
JAY275:	*MATα*	*cup1Δ RSC30*	*sfa1Δ::CORE*			
	MATa	*cup1Δ RSC30*	*sfa1Δ::CORE*			
JAY386	*MATα*	*cup1Δ RSC30*	*sfa1Δ::hisG*	*DDI1::SFA1-CUP1-HphMX4*		
	MATa	*cup1Δ RSC30*	*sfa1Δ::CORE*	*DDI1*		
JAY384:	*MATα*	*cup1Δ RSC30*	*SFA1::CUP1-HphMX4*	*DDI1::SFA1-CUP1-HphMX4*	*CAN1*	
	MATa	*cup1Δ RSC30*	*sfa1Δ::hisG*	*DDI1::SFA1-CUP1-HphMX4*	*can1Δ::NatMX4*	
JAY385:	*MATα*	*cup1Δ RSC30*	*SFA1::CUP1-HphMX4*	*DDI1::SFA1-CUP1-HphMX4*		
	MATa	*cup1Δ RSC30*	*SFA1::CUP1-HphMX4*	*DDI1::SFA1-CUP1-HphMX4*		
JAY350:	*MATα*	*cup1Δ RSC30*	*sfa1Δ::hisG*	*DDI1::SFA1-CUP1-KanMX4*	*CAN1*	
	MATa	*cup1Δ RSC30*	*sfa1Δ::hisG*	*DDI1::SFA1-CUP1-HphMX4*	*can1Δ::NatMX4*	
HSZy8 and HSZy9[c]:	*MATα*	*cup1Δ RSC30*	*sfa1Δ::hisG*	*DDI1::SFA1-CUP1-KanMX4*	*msh2Δ::hisG*	*CAN1*
	MATa	*cup1Δ RSC30*	*sfa1Δ::hisG*	*DDI1::SFA1-CUP1-HphMX4*	*msh2Δ::hisG*	*can1Δ::NatMX4*
JAY510:	*MATα*	*cup1Δ RSC30*	*sfa1Δ::hisG*	*DDI1::SFA1-CUP1-HphMX4*	*ymrcty1-5Δ::CORE*	
	MATa	*cup1Δ RSC30*	*sfa1Δ::hisG*	*DDI1::SFA1-CUP1-HphMX4*	*ymrcty1-5Δ::CORE*	

a. Only the strains ultimately used in the experiments described in the article are shown. The genotypes of the intermediate strains used in the construction of these strains are available upon request.

b. With the exception of YJM799, all strains are isogenic with MS71 and have in common the following genotype: *ade5-1*, *his7-2*, *leu2-3,112*, *LEU2*, *ura3-52*, and *trp1-289*. Only the relevant genotype modifications introduced in this study are shown in the table above.

c. HSZy1 and HSZy2, as well as HSZy8 and HSZY9, are independent strain isolates of the same genotypes, and were all used in the selection of CNV clones.

Table S1 Yeast strains used in this study (continued)

Strains[a]:	Genotypes[b]:			
Chr13 candidate fragile site mapping				
Diverged haploids:				
YJM799[d]:	*MATα*	*ho::hisG*	*ura3*	*gal2*
JAY405:	*MATa*	*cup1Δ RSC30*	*sfa1Δ::hisG*	*ADH6::CORE*
JAY794 and JAY795:	*MATa*	*cup1Δ RSC30*	*sfa1Δ::hisG*	*ura3Δ0 ADH6::CORE2*
Hybrid diploids:				
JAY408:	$\frac{MAT\alpha}{MATa}$	*cross between YJM799 and JAY405*		
JAY800 and JAY801:	$\frac{MAT\alpha}{MATa}$	*cross between YJM799 and JAY794 or JAY795, respectively*		

d. YJM799 is isogenic to YJM789, and was a generous gift from John McCusker.

Table S2 Oligonucleotide primers used in this study

Primer	5’-3’ sequence and purpose
JAO99	ACAGCATTTTACCTTTAAAAGACGTTCTCATAATACATTTTAGGATTAATACATGAGCTCGTTTTCGACACTGG For deletion of all *CUP1* repeats, Forward
JAO100	ATTTTTTGAAAAAAATGTATTACTCAAGACATTCGCTTCTAGGTCAGTCTTCATTCCTTACCATTAAGTTGATC For deletion of all *CUP1* repeats, Reverse
JAO101	ACAGCATTTTACCTTTAAAAGACGTTCTCATAATACATTTTAGGATTAATACATATGTCGGTAATGGGATCGGC For CORE removal and restoration of *RSC30*, Forward
JAO102	AAATCACATTGATAAACCTGG For CORE removal and restoration of *RSC30*, Reverse
JAO326	ATTCCGGAATTCTCAGTAGCGGTTATGAACACG For producing distal *SFA1* homology, Forward, *Eco*RI site added to 5’ end
JAO327	ATTCGCGGATCCCAAGTTGCCATTCGACTGAGG For producing distal *SFA1* homology, Reverse, *Bam*HI site added to 5’ end
JAO328	ATTCGCGGATCCACGTCCTACATTCTATCAAAT For producing proximal *SFA1* homology, Forward, *Bam*HI site
JAO329	ATTCGCGTCGACTTAGGAACAGGCGAGGTCAAT For producing proximal *SFA1* homology, Reverse, *Sal*I site added to 5’ end
JAO291	AGCTAAGGTACCTCAAGTGATGGGTACGTG Proximal to *YMRCTy1-5*, Forward, *Kpn*I site added to 5’ end
JAO294	AGCTAAGAGCTCAAGAGCAAGAGTGCAGCC Distal to *YMRCTy1-5*, Reverse, *Sac*I site added to 5’ end
JAO510	CTAATGTTTTATAAACGTTTTATGAATGACATATATGCGATAATTATATGCCTTACCATTAAGTTGATC For producing *ymrcty1-5Δ::CORE* deletion product, Forward
JAO511	GTTCCTTTTACACAACCATGATGGAACTTGCATTGATTTTTGTTGGGAGCTCGTTTTCGACACTGG For producing *ymrcty1-5Δ::CORE* deletion product, Reverse

Table S2 Oligonucleotide primers used in this study (continued)

Primer	5’-3’ sequence and purpose
JAO104	ACTAGATCTCATATGGTGATACTTTATTTC For cloning *CUP1* fragment into pAG32, Forward, *Bgl*II added to 5’ end
JAO105	ACTAGATCTCATATGTTCATGTATGTATCT For cloning *CUP1* fragment into pAG32, Reverse, *Bgl*II added to 5’ end
JAO113	AATTAAACTAAGTAAGCATGACTCAAATTTTCTGGAATACTTTGAAAATCAAATTAAGGCGCGCCAGATCT For insertion of *CUP1-Hph* downstream of *SFA1*, Forward
JAO114	CAGGTCTAACTGATTGCTGAAGAACGTAATTGTGCGCATATATATGATATTGCATAGGCCACTAGTGGATC For insertion of *CUP1-Hph* downstream of *SFA1*, Reverse
JAO143	CTGCATATTATATACTTAACAGAAGTACAATCATATACAATACAAGCATAGGCCACTAGTGGATC For insertion of *SFA1-CUP1-Hph* downstream of *DDI1*, Reverse
JAO269	TAAGTATAAGGATGTACATACTTTCATTGTTTCGTCAATTGTTGTGGTTCCATTATTATCAACTGT For insertion of *SFA1-CUP1-Hph* downstream of *DDI1*, Forward
JAO457	AGATCTGTTTAGCTTGCCTCG To produce *Kan* fragment to replace *Hph*, Forward
JAO458	GCATAGGCCACTAGTGGATCT To produce *Kan* fragment to replace *Hph*, Reverse
JAO502	TGTTAGTGTATTGATATGTGTTTCTTTTCACCTTAAAGGTGCTTAGCAAGGAGCCTTACCATTAAGTTGATC To insert CORE and CORE2 downstream of *ADH6*, Forward
JAO503	TTTTTATGATTATAAGGTACTATTTAAATATTTACAACTCGTACAGTTCTCGAGCTCGTTTTCGACACTGG To insert CORE and CORE2 downstream of *ADH6*, Reverse
JAO650	ACGTGTACAGATCTTCAATTCATCTTTTTTTTTTTTGTTCTTTTTTTTGATTCCGG *URA3* primer, used in the construction of pJA40, *Bgl*II site added to the 5’ end
JAO336	TGATGTTGTGAAGTCATTGAC *URA3* primer, used in the construction of pJA40

Table S2 Oligonucleotide primers used in this study (continued)

Primer	5'-3' sequence and purpose
JAO487	GTGGCTGTGGTTTCAGGGTCC Upstream of *URA3*, Forward, used to amplify *URA3* and repair the *ura3-52* allele
JAO490	GGCGAGGTATTGGATAGTTCC Downstream of *URA3*, Reverse, used to amplify *URA3* and repair the *ura3-52* allele
JAO863	GATGCTAAGAGATAGTGATG *URA3* primer, used to amplify the region upstream of *URA3*
JAO864	CGAGATTCCCGGGTAATAACTGCCAATCTAAGTCTGTGCTCC *URA3* primer, used to amplify the region upstream of *URA3*, overlap to JAO865
JAO865	CAGTTATTACCCGGGAATCTCG *URA3* primer, used to amplify the region downstream of *URA3*, overlap to 5' end of JAO864
JAO866	ACAGTCCTGTCTTATTGTTC *URA3* primer, used to amplify the region downstream of *URA3*
JAO1029	ACCTTAGAGTGCTCTAAGCC Used with JAO1030 to amplify the region around the *Eco*RI SNP-RFLP on Chr13
JAO1030	GCTGGTGAAACTGTATTCATT Used with JAO1029 to amplify the region around the *Eco*RI SNP-RFLP on Chr13
JAO1031	ACATTTGAGTTATTTGCTCAG Used with JAO1032 to amplify the region around the *Bgl*II SNP-RFLP on Chr13
JAO1032	CGGAAACCGTTGCATCCAACC Used with JAO1031 to amplify the region around the *Bgl*II SNP-RFLP on Chr13